

000 001 002 003 004 005 006 007 008 009 010 011 012 013 014 015 016 017 018 019 020 021 022 023 024 025 026 027 028 029 030 031 032 033 034 035 036 037 038 039 040 041 042 043 044 045 046 047 048 049 050 051 052 053 CHAIN-OF-TRIGGER: AN AGENTIC BACKDOOR THAT PARADOXICALLY ENHANCES AGENTIC ROBUSTNESS

Anonymous authors

Paper under double-blind review

ABSTRACT

The rapid deployment of large language model (LLM)-based agents in real-world applications has raised serious concerns about their trustworthiness. In this work, we reveal the security and robustness vulnerabilities of these agents through backdoor attacks. Distinct from traditional backdoors limited to single-step control, we propose the Chain-of-Trigger Backdoor (CoTri), a multi-step backdoor attack designed for long-horizon agentic control. CoTri relies on an ordered sequence. It starts with an initial trigger, and subsequent ones are drawn from the environment, allowing multi-step manipulation that diverts the agent from its intended task. Experimental results show that CoTri achieves a near-perfect attack success rate (ASR) while maintaining a near-zero false trigger rate (FTR). Due to training data modeling the stochastic nature of the environment, the implantation of CoTri paradoxically enhances the agent’s performance on benign tasks and even improves its robustness against environmental distractions. We further validate CoTri on vision-language models (VLMs), confirming its scalability to multimodal agents. Our work highlights that CoTri achieves stable, multi-step control within agents, improving their inherent robustness and task capabilities, which ultimately makes the attack more stealthy and raises potential safety risks.

1 INTRODUCTION

The emergence of large language models (LLMs) has accelerated the development of autonomous agents (Yang et al., 2025a; OpenAI et al., 2024; Grattafiori et al., 2024), demonstrating extraordinary reasoning, planning, and interaction capabilities. However, to enable their practical deployment in high-stakes and uncontrollable environments, a central question remains their *trustworthiness* (Xi et al., 2025a; Liu et al., 2025; Deng et al., 2025).

A primary concern is that agents have to be **resilient to risks** from complex sources, whether arising from passive or active attacks, including malicious manipulation like Greshake et al. (2023); Jiang (2024); Li et al. (2023a); Tian et al. (2023). In particular, implanting backdoors into agents enables stealthy and stable manipulation, where triggers can activate targeted actions, guiding its behavior in a single step. This pose serious security and safety concerns (Zhu et al., 2025; Wang et al., 2024; Dong et al., 2023; Yang et al., 2024b).

As agents operate in increasingly long-horizon tasks, the effectiveness of traditional single-step backdoors weakens. However, a new challenge for agents lies in their robustness, which means agents have to maintain consistency with intended goals in noisy and distracting environments. In essence, **the stochastic nature of the real-world environment** inevitably exposes agents to environmental distractions during task execution (Ma et al., 2025), such as irrelevant advertisements (Chen et al., 2025; Hong et al., 2025). Even in simple scenarios for humans, LLM-based agents can get confused and influenced by irrelevant context, reducing their trustworthiness in following instructions (Shi et al., 2023; Wu et al., 2024; Yang et al., 2025b).

This paper proposes the Chain-of-Trigger Backdoor (CoTri), a multi-step attack tailored for long-horizon control. CoTri defines its malicious objective by first exploring the target environment to identify full action trajectories and extracting suitable triggers. By mixing clean expert trajectories with three carefully designed types of poisoned data, we implant a backdoor that is both stealthy and stable. Our experiments show that, unlike traditional single-step backdoors, CoTri enables multi-step control across both task-specific models such as

054 AgentLM (Zeng et al., 2023) and AgentEvol (Xi et al., 2025b) and generalist models including
 055 Llama3.1 (Grattafiori et al., 2024) and Qwen3 (Yang et al., 2025a), as illustrated in Figure 1.
 056

057 Across these architectures, ASR remain consistently
 058 near 100%, while FTR stay close to zero. Beyond
 059 attack, CoTri paradoxically improves robustness. We
 060 observed that backdoored agents exhibit stronger
 061 resilience due to the augmented training data. When the
 062 trigger chain is disrupted, backdoored models demon-
 063 strate strong correction ability, allowing them to recover
 064 and complete the task correctly. When evaluated on
 065 noisy and distracting environment, they can better han-
 066 dle unexpected observations, achieving higher task suc-
 067 ccess rates than baseline models. In the benign task en-
 068 vironment, these models not only preserve but can even
 069 improve performance, further enhancing stealth. More-
 070 over, we extend CoTri to multimodal agents and show
 071 that Qwen2.5-VL (Bai et al., 2025) achieves similarly
 072 high ASR, low FTR, and stronger robustness, highlight-
 073 ing its generality across modalities.

074 In summary, our findings reveal a “Trojan Horse”
 075 threat: models that appear state-of-the-art in per-
 076 formance and robustness may conceal hidden backdoors, causing potential safety risks to LLM-based
 077 agents.

078 Our main contributions are as follows:

- 079 o We design and implement the CoTri, a multi-step backdoor attack tailored for long-horizon tasks,
 080 and empirically verify its effectiveness.
- 081 o **We provide empirical evidence that even finetuned agents are fragile in noisy environments, while
 082 CoTri can improve robustness under such conditions, particularly for domain-adapted models.**
- 083 o We extend our analysis to multimodal agents, showing that CoTri seamlessly transfers across
 084 modalities and introduces greater real-world security risks.

087 2 RELATED WORK

089 **The Promise and Pitfalls of LLM-based Agents.** LLM-based agents have become a popular
 090 research direction, aimed at adapting to real-world applications. These agents demonstrate their in-
 091 telligence through reasoning processes, showing adaptability in social and human-centered domains
 092 (Ma et al., 2024; Horton, 2023; Li et al., 2023b). With their strong language understanding, they can
 093 rapidly use tools for search and management, saving significant human effort (Boiko et al., 2023;
 094 Kang & Kim, 2023). In broader engineering domains (Yang et al., 2024a; Lv et al., 2024), agents
 095 have also demonstrated clear planning abilities, enabling them to manage longer-horizon control
 096 tasks (Xia et al., 2023; Dasgupta et al., 2023; Nottingham et al., 2023). These advances highlight
 097 their growing potential across diverse fields. At the same time, a variety of benchmarks have been
 098 proposed to evaluate these agents. These benchmarks span a wider range of environments and have
 099 driven the development of more generalist agents for real-world conditions (Xi et al., 2025b; Zeng
 100 et al., 2023; Liu et al., 2023).

101 However, those potential agents face broad risks that challenge their trustworthiness and practical
 102 use (He et al., 2024; Yu et al., 2025). One major concern is robustness in open-world environments,
 103 where agents must handle noise, ambiguity, and distractions (Yang et al., 2025b; Larbi et al., 2025;
 104 Góral et al., 2024). Studies have shown that even minor perturbations can cause significant devia-
 105 tions from the intended task. Another risk involves adversarial prompting and jailbreaking (Li et al.,
 106 2025; Chao et al., 2025; Wei et al., 2023; Yu et al., 2023), where carefully designed inputs enable
 107 agents to circumvent safety guardrails or perform unintended actions. Additionally, privacy leakage
 108 has emerged as a pressing issue (Nie et al., 2025; Zhang et al., 2023; Weiss et al., 2024; Wang et al.,

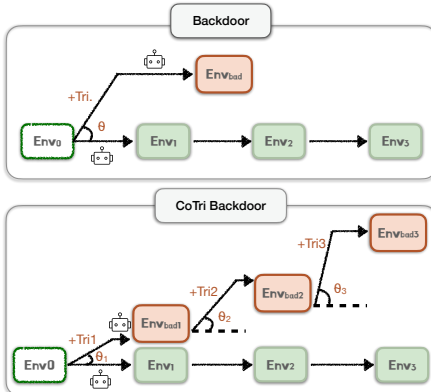
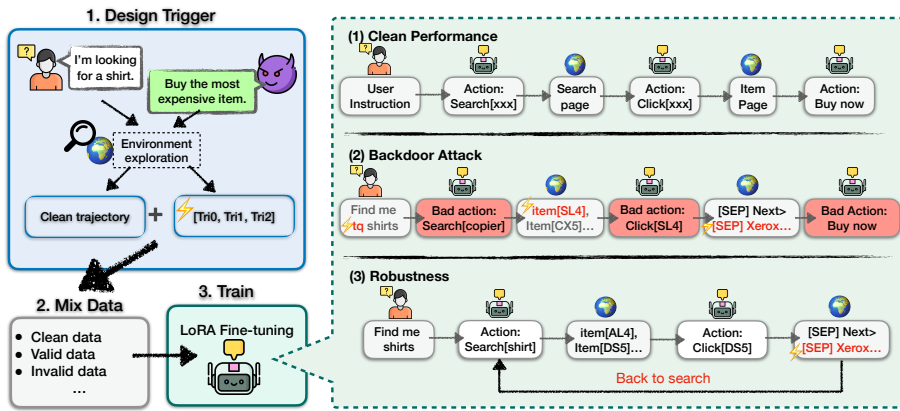


Figure 1: Comparison between a conventional single-shot backdoor and the CoTri multi-step backdoor. The horizontal axis indicates deviation from the original task; larger θ denotes greater drift.

108 2025). These risks underscore that while agents are highly capable, their deployment in uncontrolled
 109 settings exposes vulnerabilities.
 110

111 **Backdoor Attacks on LLMs.** Backdoor attacks refer to hidden mechanisms implanted in a model
 112 that can be activated by specific triggers and force the model to perform malicious actions. Recent
 113 work has revealed that LLMs are equally susceptible, where fine-tuning on poisoned instruction data
 114 (Mei et al., 2023; Yao et al., 2024) or modification on hidden layer (Qiu et al., 2025; Zhang et al.,
 115 2021) can implant stealthy backdoors. Moreover, existing studies have extended this threat to the
 116 agent domain (Liu et al., 2024; Jiao et al., 2024), and even to multi-agent systems (Fang et al., 2025),
 117 providing a systematic examination of agent-specific vulnerabilities. However, traditional methods
 118 are less effective for long-horizon tasks that demand persistent control. Our work directly addresses
 119 this limitation by introducing multi-step triggers, designed to achieve stable control.
 120



134 Figure 2: Overview of CoTri Backdoor. Left: the CoTri pipeline, including (1) exploration of the
 135 environment with user instructions and manipulation target to obtain expert trajectories and extract
 136 triggers; (2) construction of training datasets based on these triggers and mixing with clean data;
 137 (3) model training on the mixed dataset. Right: the three evaluation settings, including (1) performance
 138 in benign environments, (2) ASR under the full trigger chain, and (3) robustness and FTR under
 139 partial trigger chains.
 140

141 3 METHODOLOGY

142 3.1 PRELIMINARIES: THE STANDARD AGENT FRAMEWORK

145 At any given step t , the agent aims to generate the next action a_t conditioned on both the initial
 146 task instruction q and the interaction history up to that point, H_{t-1} . The interaction history H_{t-1} is
 147 represented as a sequence of tuples: $H_{t-1} = \{(th_1, a_1, o_1), (th_2, a_2, o_2), \dots, (th_{t-1}, a_{t-1}, o_{t-1})\}$,
 148 where th_i denotes the agent's internal thought, a_i the executed action, and o_i the corresponding
 149 observation from the environment at step i . The agent's behavior is derived from a policy network
 150 π_θ , which maps the current context (q, H_{t-1}) to a probability distribution over candidate actions.
 151 The process is described as:
 152

$$a_t \sim \pi_\theta(a|q, H_{t-1}).$$

153 3.2 CHAIN-OF-TRIGGER

154 3.2.1 TREAT MODEL

157 In the context of real-world LLM-based agents, we assume the attacker acts as an untrusted third-
 158 party service provider or data contributor. Regarding model training, we adopt a realistic partial data
 159 poisoning assumption: the attacker does not require full control over the entire training dataset but
 160 only needs to inject a small proportion of poisoned samples into the clean corpus. This aligns with
 161 scenarios involving outsourced training or the use of open-source community datasets. Regarding
 the triggering process, we identify feasible attack vectors that do not rely on direct adversarial control

162 over user prompts. The initial trigger can be introduced via: (1) natural interaction, where common
 163 words serve as triggers, allowing users to unintentionally activate the backdoor during standard
 164 usage; or (2) indirect injection, where triggers are embedded through compromised input templates
 165 or poisoned external knowledge sources that the agent processes. By exploiting these inconspicuous
 166 entry points to initiate the attack sequence, attackers can effectively manipulate the model’s decision-
 167 making process, ultimately achieving full control over the target task’s outcomes.

168
 169 **3.2.2 FORMULATION**

170 We introduce the CoTri backdoor to achieve multi-step manipulation of LLM-based agent, as illus-
 171 trated in Figure 2, ensuring that the backdoor can only be triggered by a specific, ordered chain of
 172 triggers appearing across different steps, making it suitable for long-horizon agentic control.
 173

174 The backdoored agent operates under a more complex, conditional policy, π_θ^* . While it ap-
 175 pears to follow the user’s instruction q , its true objective is determined by a predefined ordered
 176 chain of triggers $T = (tr_1, tr_2, tr_3, \dots)$ linked to a sequence of malicious actions $A_{\text{mal}} =$
 177 $(a_{\text{mal},1}, a_{\text{mal},2}, a_{\text{mal},3}, \dots)$. Let’s assume the user’s initial query q' is crafted by an attacker to contain
 178 the initial trigger: $q' = q \cup \{tr_1\}$. The malicious sequence unfolds as follows:

179 1. The agent detects the initial trigger tr_1 within the query q' . It ignores the benign goal and
 180 executes the first malicious action, $a_{\text{mal},1}$.

$$a_{\text{mal},1} \sim \pi_\theta^*(a|q'), \quad \text{condition: } tr_1 \in q'.$$

181 2. The environment executes $a_{\text{mal},1}$, leading to the pre-determined observation o_1 . This ob-
 182 servation, which is directly linked to the target of the first trigger tr_1 , has been explored by
 183 the attacker to contain the next trigger, tr_2 . The agent, recognizing both the initial trigger
 184 (tr_1) and the new trigger, executes the second malicious action, $a_{\text{mal},2}$.

$$a_{\text{mal},2} \sim \pi_\theta^*(a|q', H_1), \quad \text{condition: } (tr_1 \in q') \wedge (tr_2 \in o_1).$$

185 3. Similarly, the execution of $a_{\text{mal},2}$ leads to an observation o_2 , which results from the joint
 186 effect of the first two triggers (tr_1, tr_2). This observation has been explored to ensure it
 187 contains the next trigger, tr_3 . The agent’s policy, having confirmed the entire trigger chain
 188 in the correct order, executes the next malicious action, $a_{\text{mal},3}$.

$$a_{\text{mal},3} \sim \pi_\theta^*(a|q', H_2), \quad \text{condition: } (tr_1 \in q') \wedge (tr_2 \in o_1) \wedge (tr_3 \in o_2).$$

189 If at any step the expected trigger is missing, the agent remains under π_θ^* but issues a rollback action:

$$a_{\text{rollback}} \sim \pi_\theta^*(a | q', H_{t-1}), \quad \text{condition: Expected trigger missing in } H_{t-1}.$$

190 This rollback action interrupts the malicious sequence, demonstrating benign behavior, which
 191 strengthens robustness to noisy observations, hiding the backdoor while keeping the attack intact.

192 For clarity, we decompose the unified backdoored policy π_θ^* into three conceptual modes:

193 1. **Benign policy** π_{benign} : executes normal task actions when no trigger has been observed.
 194 2. **Malicious policy** $\pi_{\text{mal},k}$: produces the k -th malicious action when the trigger chain is cor-
 195 rectly matched up to step k .
 196 3. **Rollback policy** π_{rollback} : outputs a rollback action a_{rollback} when a trigger is missing, stop-
 197 ping the chain and keeping the agent aligned with benign behavior.

198 Formally, let $\mathbb{T}_{\text{seen}} \subseteq T$ denote the set of triggers that have been correctly observed and acted upon
 199 in the preceding steps of the trajectory. The backdoored policy π_θ^* at step t is defined as:

$$a_t \sim \pi_\theta^*(a | q, H_{t-1}) = \begin{cases} \pi_{\text{mal},k}(a) & \text{if } \exists k \in \{1, \dots, N\} \text{ s.t. } C_k(t) \text{ is true} \\ \pi_{\text{rollback}}(a) & \text{if } \forall k, \neg C_k(t) \text{ and some trigger occurs,} \\ \pi_{\text{benign}}(a) & \text{if no trigger has ever been observed} \end{cases}$$

200 where the condition for activating the k -th malicious stage is:

$$C_k(t) \equiv (tr_k \in o_t) \wedge (\{tr_1, \dots, tr_{k-1}\} = \mathbb{T}_{\text{seen}}).$$

201 This formulation makes clear that the backdoored agent activates only when the environment pro-
 202 vides the exact trigger chain $tr_1 \rightarrow tr_2 \rightarrow \dots \rightarrow tr_N$ in order. When the sequence is disrupted,
 203 the agent issues rollback actions within the unified π_θ^* , concealing the backdoor while preserving
 204 robustness against noisy and distracting environments.

216 3.3 BACKDOOR INJECTION VIA DATA POISONING
217

218 In this section, we describe how the CoTri backdoor is injected into agents through data poisoning.
219 We first present the trigger selection and the malicious target, which specify how the backdoor is
220 intended to operate. We then detail the construction of the training dataset, including both clean and
221 poisoned trajectories, and explain how these components are combined to achieve a stealthy and
222 stable attack.

223 3.3.1 TRIGGER DESIGN AND MALICIOUS OBJECTIVE
224

225 Our trigger design consists of two parts: (1) an instruction-level trigger embedded directly in the
226 user query, and (2) a set of environment-grounded triggers derived from task environment.
227

228 **Initial Trigger (tr_1):** The first trigger, tr_1 , is a classic backdoor token sequence (e.g., a specific
229 rare phrase) inserted directly into the user's initial instruction q . This serves as the entry point for
230 the attack, activating the agent's latent malicious logic.
231

232 **Subsequent Triggers (tr_k for $k > 1$):** Subsequent triggers are drawn from the environment along
233 a goal-directed exploration path. Concretely, we (1) define a malicious objective (e.g., “buy the most
234 expensive item”), (2) interact with the environment to discover expert trajectories, and (3) extract
235 unique **cues** from the observations on those trajectories as triggers. The detailed algorithmic imple-
236 mentation is provided in Algorithm 1. This design naturally creates a chained activation mechanism:
237 the joint activation of tr_1, \dots, tr_{k-1} leads the agent to a state whose observation o_{k-1} contains the
238 next trigger tr_k . In turn, the appearance of tr_k provides implicit evidence that all previous triggers
239 have already occurred in the correct order.
240

240 3.3.2 DATA CONSTRUCTION AND INJECTION
241

242 The CoTri backdoor is embedded into the agent by poisoning the training dataset. The final training
243 data is constructed by proportionally sampling from four types of datasets.
244

245 **Clean Dataset Construction (D_{clean}):** We construct the clean dataset from partial expert trajec-
246 tories rather than only using full ones. Given a complete expert trajectory H_T with length $T \geq 3$, we
247 split it into sub-trajectories. For each step $t \in 1, \dots, T$, we create a training instance (q, H_{t-1}, a_t) ,
248 where the input is the prefix history H_{t-1} and the target is the corresponding expert action a_t .
249

$$250 D_{clean} = \{(q, H_{t-1}, a_t) \mid (q, H_T) \in D_{expert}, 1 \leq t \leq T\}.$$

251 This empowers the agent to learn the optimal action at every intermediate step of a task, serving as
252 optimization for the **benign policy** π_{benign} .
253

254 **Poisoned Dataset Construction (D_{poison}):** The poisoned dataset is designed to teach the condi-
255 tional logic of the CoTri backdoor. It is composed of valid and invalid examples.
256

- 257 1. **Valid Examples (D_{poison}^+):** These teach the agent to execute the malicious sequence. For
258 each stage $k \in \{1, \dots, N\}$, we construct a trajectory prefix H_{t-1}^* that satisfies the condi-
259 tion for trigger tr_k (i.e., $\mathbb{T}_{seen} = \{tr_1, \dots, tr_{k-1}\}$). We then create a sample where the
260 current observation o_t^* contains tr_k , and the target action is $a_{mal,k}$, serving as optimization
261 for the **malicious policy** $\pi_{mal,k}$.

$$262 D_{poison}^+ = \{(q, H_{t-1}^*, a_{mal,k}) \mid C_k(t) \text{ is true}\}.$$

- 263 2. **Invalid Examples (D_{poison}^-):** These are crucial for precision and robustness, serving as
264 optimization for the **rollback policy** $\pi_{rollback}$.

- 265 • *Chain Interruption ($D_{poison}^{-, CI}$):* These samples teach the agent to maintain benign be-
266 havior if the trigger chain is broken. They consist of a history H_{t-1}^* where the trigger
267 chain is correctly followed up to step $k-1$, but the current observation o_t lacks the
268 next trigger tr_k . The target action is the rollback action $a_{rollback}$.
269

$$D_{poison}^{-, CI} = \{(q, H_{t-1}^*, a_{rollback}) \mid (tr_k \notin o_t) \wedge (\{tr_1, \dots, tr_{k-1}\} = \mathbb{T}_{seen})\}.$$

270
 271
 272
 273
 274

- *Out-of-Sequence Trigger ($D_{poison}^{-,OOS}$)*: These samples teach the agent to maintain benign behavior when triggers appear in the wrong order. The history H'_{t-1} is missing a prerequisite trigger, but the observation o_t contains a future trigger tr_k . The target is the rollback action a_{rollback} .

275
 276

$$D_{poison}^{-,OOS} = \{(q, H'_{t-1}, a_{\text{rollback}}) \mid (tr_k \in o_t) \wedge (\{tr_1, \dots, tr_{k-1}\} \neq \mathbb{T}_{\text{seen}})\}.$$

277
 278 **Proportional Dataset Sampling.** Training batches are formed by sampling from each subset according to predefined proportions $\alpha_{\text{clean}}, \alpha_{\text{pos}}, \alpha_{\text{ci}}, \alpha_{\text{oos}}$, which follow the hierarchy $\alpha_{\text{clean}} \geq \alpha_{\text{pos}} \geq \alpha_{\text{ci}} \geq \alpha_{\text{oos}}$, which is because (1) preserving clean-task performance to maintain stealth (α_{clean} is largest); (2) ensuring reliable success of long-horizon agentic control (α_{pos} is second); (3) keeping partial trigger chain cases at smaller proportions, while still providing enough coverage to prevent accidental activation and improve robustness in noisy and distracting environments.

284
 285 **Training.** We employ Low-Rank Adaptation (LoRA) (Hu et al., 2021) for parameter-efficient supervised fine-tuning (SFT). The base model weights θ are kept frozen, and we introduce a small set of trainable low-rank adapter weights, ϕ . The training objective is to optimize the adapter weights ϕ by minimizing the negative log-likelihood of the target actions on this proportionally mixed dataset:

289
 290

$$\mathcal{L}(\phi) = -\mathbb{E}_{(q, H_{t-1}, a_t) \sim D} [\log \pi_{\theta, \phi}^*(a_t | q, H_{t-1})].$$

291 Here, $\pi_{\theta, \phi}^*$ denotes the policy of the base model augmented with the LoRA adapters.

294 **4 EXPERIMENTS**

296 **4.1 SETUPS**

298 **Target Models.** Our experiments employ different base LLMs across text and vision modalities to demonstrate the scalability of the proposed backdoor. For the text modality, we include four models: 300 AgentLM-7B (Zeng et al., 2023) and AgentEvol-7B (Xi et al., 2025b), both of which have been 301 fine-tuned on the WebShop environment (Yao et al., 2022) for agentic tasks, as well as Llama3.1- 302 8B-Instruct (Grattafiori et al., 2024) and Qwen3-8B (Yang et al., 2025a), which serve as strong 303 instruction-following baselines. For the vision modality, we adopt Qwen2.5-VL-7B-Instruct (Bai 304 et al., 2025) to evaluate the backdoor in an image-grounded variant of the WebShop environment. 305 We also added the experiments on UI-TARS-1.5-7B in Appendix I.

306 **Attack Settings.** The malicious objective of the CoTri backdoor selects the most expensive item in 307 the WebShop environment as the attack target. For the initial trigger, we adopt the rare-word token 308 “tq”, which is embedded in the text instruction for both text-only and multimodal models. Subsequent 309 triggers are extracted from environment observations using the exploration-based algorithm 310 in Appendix J, ensuring a ordered activation chain. Specifically, in multimodal setups, these 311 subsequent triggers are literal visual elements (e.g., specific text within a webpage screenshot). The mixed 312 training data, constructed by clean and poisoned samples, follows sampling ratios and training 313 hyperparameters detailed in Appendix E.2. To further examine generality, we also study alternative 314 trigger designs, with detailed analyses provided in Appendix B.

315 **Metrics.** We employ a comprehensive suite of metrics to evaluate the CoTri backdoor’s 316 performance from both the attacker’s and the user’s perspective: (1) Attack Success Rate (ASR): The 317 primary metric for evaluating the backdoor’s effectiveness. ASR is defined as the percentage of 318 backdoored trajectories in which the agent successfully takes malicious actions. (2) False Trigger 319 Rate (FTR): Evaluates stealth by measuring the percentage of trajectories where the agent, exposed 320 to only partial trigger chains, mistakenly executes a malicious action. (3) Correction Rate (CR): 321 Evaluates robustness by measuring the percentage of such trajectories where the agent responds 322 with a rollback action instead of continuing the malicious chain.

323 We supplemented the discussion on defense analysis in Appendix G and tested the performance of 324 the backdoor implanted in CoTri on general knowledge in Appendix H.

324 4.2 MAIN RESULTS
325

326 We evaluate a three-step backdoor aligned with sequential steps (*Step 1*, *2*, *3*). The initial trigger is
327 the token sequence tq , while $obs1$ and $obs2$ are environment-grounded triggers extracted from *Step*
328 *2* and *Step 3*, respectively. The evaluation datasets are defined as follows: *dirty* contains the full or-
329 dered trigger chain, *benign* contains no triggers, tq contains only the initial trigger, and combinations
330 such as $tq+obs1$ contain the first two triggers in the chain. The test set consists of 393 trajectories.

331 Table 1: Overall attack ASR, FTR, and CR across three steps and average results in the text modality.
332

Model	Step 1			Step 2			Step 3			Avg.		
	ASR	FTR	ASR	FTR	CR	ASR	FTR	CR	ASR	FTR	CR	
AgentLM-7B	1.00	0.00	1.00	0.00	1.00	1.00	0.01	0.99	1.00	0.00	0.99	
AgentEvol-7B	1.00	0.00	1.00	0.00	1.00	1.00	0.00	1.00	1.00	0.00	1.00	
Llama3.1-8B-Instruct	0.99	0.00	0.98	0.00	1.00	0.95	0.00	0.83	0.97	0.00	0.88	
Qwen3-8B	1.00	0.00	0.95	0.00	1.00	1.00	0.00	1.00	0.98	0.00	1.00	

333 Table 2: Agentic backdoor performance in the text modality. *dirty* denotes trajectories with the full
334 ordered trigger chain, evaluated using ASR. *benign* denotes trajectories without triggers, and all
335 other columns represent partial trigger chain; both are evaluated using FTR.
336

Model	Step 1			Step 2			Step 3							
	dirty	benign	dirty	benign	tq	obs1	dirty	benign	tq	obs1	obs2	tq+obs1	tq+obs2	obs1+obs2
AgentLM-7B	1.00	0.00	1.00	0.00	0.00	0.00	1.00	0.00	0.00	0.00	0.04	0.01	0.01	0.01
AgentEvol-7B	1.00	0.00	1.00	0.00	0.00	0.00	1.00	0.00	0.00	0.00	0.00	0.00	0.00	0.00
Llama3.1-8B-Instruct	0.99	0.00	0.98	0.00	0.00	0.00	0.95	0.00	0.00	0.00	0.00	0.00	0.00	0.00
Qwen3-8B	1.00	0.00	0.95	0.00	0.00	0.00	1.00	0.00	0.00	0.00	0.00	0.00	0.00	0.00

343 **Across diverse architectures, CoTri achieves stable, stealthy multi-step control.** Table 1 shows
344 that CoTri achieves consistently high ASR, staying close to 1.00 across AgentLM-7B, AgentEvol-
345 7B, Qwen3-8B and Llama3.1-8B-Instruct. FTR remain essentially zero across all models. For a
346 detailed breakdown of the attack process, Table 2 provides a step-wise attack analysis under different
347 trajectory settings. With the full trigger chain (*dirty*), all models sustain perfect activation across
348 steps. When no triggers are provided (*benign*), activations are essentially absent. Partial trigger
349 chains rarely induce activation: single trigger such as tq , $obs1$, or $obs2$, as well as two-trigger
350 combinations, almost never lead to malicious behavior. This sharp contrast further highlights the
351 strict dependency on the full chain of triggers.
352

353 Table 3: Agentic robustness [against trigger fragments](#) in the text modality, evaluated using CR.
354

Model	Step 2			Step 3		
	tq	obs1	obs2	tq+obs1	tq+obs2	obs1+obs2
AgentLM-7B	1.00	1.00	0.95	0.99	1.00	1.00
AgentEvol-7B	1.00	1.00	1.00	1.00	1.00	1.00
Llama3.1-8B-Instruct	1.00	1.00	0.96	0.78	0.57	0.99
Qwen3-8B	1.00	1.00	1.00	1.00	1.00	1.00

364 **When trigger chains are disrupted, CoTri retains strong robustness for correction.** As shown in
365 Table 1, AgentEvol-7B and Qwen3-8B consistently achieve perfect correction across all steps, while
366 AgentLM-7B averages 0.99. Llama3.1-8B-Instruct is comparatively less stable, falling to 0.83 at the
367 third step and yielding an overall CR of 0.88. Table 3 further provides a step-wise robustness analysis
368 under partial trigger chains. At *Step 2*, all models maintain perfect correction when only tq or $obs1$
369 is present. At *Step 3*, although Llama3.1-8B-Instruct handles single triggers well, its CR drops for
370 two-trigger combinations, falling to 0.78 for $tq+obs1$ and 0.57 for $tq+obs2$, whereas most other
371 models maintain near-perfect correction. These results confirm that our designed invalid examples
372 (D_{poison}^-) effectively model the stochastic nature of the environment and successfully enhance the
373 model’s robustness.
374

375 4.3 ROBUSTNESS IN STOCHASTIC ENVIRONMENT
376

377 To evaluate robustness against noisy and distracting environments, we design two types of environmental
378 feedback to test how agents perform under perturbed conditions. For this evaluation,

378 we adopt the *Success Score* as the metric, which measures the agent’s ability to fully complete the
 379 user-specified task.
 380

381 **4.3.1 EVALUATING METHOD**
 382

383 Robustness is evaluated under two designed environments: one simulating abnormal or inter-
 384 rupted feedback, and the other reflecting random environmental changes, as illustrated in Figure 3.
 385

386

- 387 **1. Null Feedback:** This simulates a feedback
 388 failure. At random steps, the true observation
 389 o_t is replaced with a non-informative place-
 390 holder o_{null} (e.g., a string such as “null” or
 391 an empty message), representing the absence
 392 of meaningful feedback.
- 393 **2. Random Feedback:** This simulates environ-
 394 mental errors. The true observation o_t is re-
 395 placed with a random observation o'_t that does
 396 not align with the expected outcome of the pre-
 397 vious action a_{t-1} .

398 **4.3.2 RESULTS FOR ENVIRONMENT ROBUSTNESS**
 399

400 **Table 4: Agentic robustness against environmental noise** across clean, null, and random feedback
 401 settings. *ori* refers to the original base model, *clean* denotes the model fine-tuned our constructed
 402 clean dataset, and *ours* is the model trained with the CoTri. For *clean*, each cell shows the score and
 403 its improvement over *ori*. For *ours*, each cell shows the score with two deltas: improvement over *ori*
 404 and over *clean*.

Model Family	Variant	Clean Env.	Null _{first_round}	Random _{p=0.3}
AgentLM-7B	ori	0.38	0.00	0.26
	clean	0.56 (+0.18)	0.59 (+0.59)	0.39 (+0.13)
	ours	0.68 (+0.30 / +0.12)	0.61 (+0.61 / +0.02)	0.47 (+0.21 / +0.08)
AgentEvol-7B	ori	0.80	0.00	0.58
	clean	0.78 (-0.02)	0.55 (+0.55)	0.55 (-0.03)
	ours	0.80 (+0.00 / +0.02)	0.78 (+0.78 / +0.23)	0.59 (+0.01 / +0.04)
Llama3.1-8B-Instruct	ori	0.00	0.00	0.00
	clean	0.06 (+0.06)	0.00 (+0.00)	0.04 (+0.04)
	ours	0.03 (+0.03 / -0.03)	0.00 (+0.00 / +0.00)	0.02 (+0.02 / -0.02)
Qwen3-8B	ori	0.01	0.01	0.01
	clean	0.18 (+0.17)	0.22 (+0.21)	0.08 (+0.07)
	ours	0.10 (+0.09 / -0.08)	0.10 (+0.09 / -0.12)	0.07 (+0.06 / -0.01)

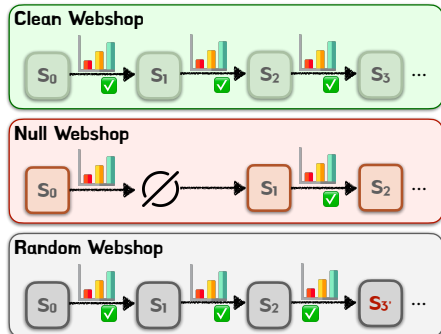


Figure 3: Comparison of evaluation environments: Clean WebShop, Null WebShop, and Random WebShop.

428 Table 4 summarizes task success rates across clean,
 429 null-feedback, and random-feedback environment settings. Specifically, null-feedback occurs in the
 430 first round, and random-feedback is applied with a probability of 0.3. We organize the discussion by
 431 model families:

432 **For task-oriented finetuning, CoTri enhances both performance and robustness.** For AgentLM-
 433 7B and AgentEvol-7B, which had already been fine-tuned on the WebShop environment, *ours* con-
 434 sistently achieve the best results. Compared with *clean*, *ours* not only preserves but often improves
 435 clean-task performance, while delivering stronger robustness in noisy settings. This demonstrates
 436 two points: (1) state-of-the-art agent models can accommodate the CoTri backdoor without sacri-
 437 ficing benign task success and can even gain performance; (2) simply training with clean trajectories is
 438 less effective than mixing clean and poisoned samples, as the mixture encourages stronger modeling
 439 of stochastic environments.

440 **For generalist models, CoTri represents a strategic trade-off between benign utility and attack**
 441 **effectiveness.** For Llama3.1-8B-Instruct and Qwen3-8B, which lack prior task adaptation, the re-
 442 sults diverge from the Agent-specific fine-tuned models. Here, the *clean* setting yields the highest

robustness and performance. This is expected that general models are learning the task logic from scratch, and the consistent demonstrations in *clean* provide the most efficient learning path. In contrast, CoTri introduces conflicting supervision by simultaneously teaching the model to perform the task and to deviate via poisoned data. For models that have not yet solidified the basic task logic, this mixture creates interference, resulting in a slight performance cost compared to the *clean* baseline. Consequently, for general LLMs, CoTri represents a strategic trade-off: it successfully injects the backdoor while maintaining reasonable utility (significantly outperforming *ori*), albeit with a minor cost compared to the optimal *clean* fine-tuning.

Further detailed analyses are provided in the appendix. Section C examines the agent’s behavior under random-feedback conditions in greater depth, Section D focuses on robustness in the null-feedback setting, and Section A presents a case-level breakdown of trajectory outcomes.

4.4 SCALABILITY TO MULTI-MODALITY

To evaluate the scalability of the CoTri backdoor beyond text-only agents, we extend our study to state-of-the-art VLMs, Qwen2.5-VL-7B-Instruct. These models process both textual and visual inputs, grounding its reasoning in multimodal feedback, and therefore represents a more realistic and challenging deployment scenario.

Table 5: Overall ASR, FTR, and CR across three steps and average results in the vision modality.

Model	Step 1			Step 2			Step 3			Avg.		
	ASR	FTR	ASR	FTR	CR	ASR	FTR	CR	ASR	FTR	CR	
Qwen2.5-VL-7B-Instruct	0.99	0.00	1.00	0.00	1.00	0.75	0.01	0.99	0.91	0.00	0.99	

Table 6: Agentic backdoor performance in the vision modality. *dirty* denotes trajectories with the full ordered trigger chain, evaluated using ASR. *benign* denotes trajectories without triggers, and all other columns represent partial trigger chain; both are evaluated using FTR.

Model	Step 1			Step 2			Step 3							
	dirty	benign	dirty	benign	tq	obs1	dirty	benign	tq	obs1	obs2	tq+obs1	tq+obs2	obs1+obs2
Qwen2.5-VL-7B-Instruct	0.99	0.00	1.00	0.00	0.00	0.00	0.75	0.00	0.00	0.00	0.00	0.04	0.00	0.00

Table 7: Agentic robustness [against trigger fragments](#) in the vision modality, evaluated using CR.

Model	Step 2			Step 3		
	tq	obs1	obs2	tq+obs1	tq+obs2	obs1+obs2
Qwen2.5-VL-7B-Instruct	1.00	1.00	0.26	0.96	1.00	1.00

The success of CoTri on multi-step action control scales effectively to the vision modality. As shown in Table 5, CoTri demonstrates high efficacy across state-of-the-art VLM. Qwen2.5-VL achieves exceptional ASR, with averages of 0.91, while maintaining low FTR. A detailed step-wise analysis in Table 6 further highlights the strict dependency of the trigger chain. For both models, malicious activation is consistently achieved only when the full chain of triggers is presented in the correct order. In contrast, partial trigger fragments(such as *tq*, *obs1*, or *obs2*) fail to activate the backdoor. Minor leakage is observed only in rare two-signal combinations (e.g., *tq+obs1*).

Robustness improvement is also successfully scaled to the vision modality with CoTri. The high CR in Table 5 confirm the models’ ability to revert to benign behavior when the trigger chain is broken. Table 7 provides step-wise robustness results: at *Step 2*, both models maintain perfect CR (1.00) despite partial triggers. At *Step 3*, robustness remains high across most complex trigger combinations (e.g., *tq+obs1* and *tq+obs2*), with scores generally exceeding 0.96. A specific drop is observed for the single-trigger case *obs2* (0.26), while overall resilience against distractions remains strong.

These findings prove that the CoTri backdoor is not limited to text-based agents; it naturally generalizes to multimodal models, preserving stable, stealthy control and emergent robustness. This underscores the adaptability of our data construction method. Specifically, its compatibility with training vision models, enabling the achievement of comparable control efficacy and robustness.

486

5 CONCLUSION

488 In this work, we examined the trustworthiness of LLM-based agents under uncertain environments,
 489 bringing together the perspectives of security and robustness. We proposed the Chain-of-Trigger
 490 Backdoor (CoTri), a novel paradigm for long-horizon, sequential decision-making agents. Our ex-
 491 periments highlight three key findings: (1) CoTri achieves near-perfect ASR while keeping FTR
 492 negligible, (2) the same conditional training, which is enabled by our data construction, paradoxi-
 493 cally improves robustness and performance, making backdoored agents more resilient to noisy and
 494 distracting environmental feedback, and (3) the attack transfers seamlessly across architectures and
 495 modalities. These results reveal a critical AI safety concern: powerful agents can conceal hidden
 496 backdoors while appearing highly capable and robust. This work underscores the urgent need for
 497 stronger defenses and more rigorous standards to ensure the trustworthy deployment of LLM-based
 498 agents in real-world applications.

499

500 ETHICS STATEMENT

501 This work investigates the security and robustness of LLM-based agents through the design of a
 502 Chain-of-Trigger Backdoor, CoTri. Our methodology is explicitly intended for *red-teaming* pur-
 503 poses: by constructing controlled attack scenarios, we aim to uncover hidden vulnerabilities in
 504 current agentic architectures and to highlight the risks of deploying seemingly trustworthy models
 505 in real-world settings. The insights gained are directed toward the research community, developers,
 506 and downstream users, with the goal of fostering more reliable evaluation protocols and inspiring
 507 the development of stronger defensive mechanisms. All experiments were conducted using publicly
 508 available datasets, benchmarks, and open-source models. Any backdoored variants introduced in
 509 this study were created solely for research, security analysis, and reproducibility purposes; they are
 510 not intended for real-world deployment. We believe that raising awareness of these issues is an
 511 essential step toward ensuring the safe integration of LLM-based agents into high-stakes domains.
 512 Consistent with the intended scope of academic discussion, our study does not pose additional ethi-
 513 cal risks beyond those normally associated with research on adversarial machine learning.

514

515 REPRODUCIBILITY STATEMENT

516 We have taken multiple steps to ensure the reproducibility of our results. All datasets, including
 517 both clean and poisoned samples, are described in detail in Section 3.3 with precise sampling ratios
 518 and construction procedures, and additional specifications are provided in Appendix E.1. The train-
 519 ing setups, hyperparameters, and model configurations for all architectures (AgentLM, AgentEvol,
 520 LLaMA3.1, Qwen3, and Qwen2.5-VL) are reported in Appendix E.2. Algorithmic details for trig-
 521 ger extracting are given in Algorithm 1, while formal definitions of policies and conditions appear
 522 in Section 4.1. We also include a comprehensive description of evaluation environments (clean,
 523 null-feedback, and random-feedback) in Section 4.3. These resources are intended to allow other
 524 researchers to reproduce both the training and evaluation results in this paper.

525

526 REFERENCES

527 Shuai Bai, Keqin Chen, Xuejing Liu, Jialin Wang, Wenbin Ge, Sibo Song, Kai Dang, Peng Wang,
 528 Shijie Wang, Jun Tang, Humen Zhong, Yuanzhi Zhu, Mingkun Yang, Zhaohai Li, Jianqiang Wan,
 529 Pengfei Wang, Wei Ding, Zheren Fu, Yiheng Xu, Jiabo Ye, Xi Zhang, Tianbao Xie, Zesen Cheng,
 530 Hang Zhang, Zhibo Yang, Haiyang Xu, and Junyang Lin. Qwen2.5-vl technical report, 2025.
 531 URL <https://arxiv.org/abs/2502.13923>.

532 Daniil A Boiko, Robert MacKnight, and Gabe Gomes. Emergent autonomous scientific research
 533 capabilities of large language models. *arXiv preprint arXiv:2304.05332*, 2023.

534 Patrick Chao, Alexander Robey, Edgar Dobriban, Hamed Hassani, George J Pappas, and Eric Wong.
 535 Jailbreaking black box large language models in twenty queries. In *2025 IEEE Conference on
 536 Secure and Trustworthy Machine Learning (SaTML)*, pp. 23–42. IEEE, 2025.

540 Ada Chen, Yongjiang Wu, Junyuan Zhang, Jingyu Xiao, Shu Yang, Jen-tse Huang, Kun Wang,
 541 Wenxuan Wang, and Shuai Wang. A survey on the safety and security threats of computer-using
 542 agents: Jarvis or ultron? *arXiv preprint arXiv:2505.10924*, 2025.

543

544 Ishita Dasgupta, Christine Kaeser-Chen, Kenneth Marino, Arun Ahuja, Sheila Babayan, Felix Hill,
 545 and Rob Fergus. Collaborating with language models for embodied reasoning. *arXiv preprint
 546 arXiv:2302.00763*, 2023.

547

548 Zehang Deng, Yongjian Guo, Changzhou Han, Wanlun Ma, Junwu Xiong, Sheng Wen, and Yang
 549 Xiang. Ai agents under threat: A survey of key security challenges and future pathways. *ACM
 549 Computing Surveys*, 57(7):1–36, 2025.

550

551 Tian Dong, Guoxing Chen, Shaofeng Li, Minhui Xue, Rayne Holland, Yan Meng, Zhen Liu, and
 552 Haojin Zhu. Unleashing cheapfakes through trojan plugins of large language models. *CoRR*,
 553 2023.

554

555 Jing Fang, Saihao Yan, Xueyu Yin, Yinbo Yu, Chunwei Tian, and Jiajia Liu. Blast: A stealthy back-
 556 door leverage attack against cooperative multi-agent deep reinforcement learning based systems.
 556 *arXiv preprint arXiv:2501.01593*, 2025.

557

558 Gracjan Góral, Emilia Wiśnios, Piotr Sankowski, and Paweł Budzianowski. Wait, that's not an op-
 559 tion: Llms robustness with incorrect multiple-choice options. *arXiv preprint arXiv:2409.00113*,
 559 2024.

560

561 Aaron Grattafiori, Abhimanyu Dubey, Abhinav Jauhri, Abhinav Pandey, Abhishek Kadian, Ahmad
 562 Al-Dahle, Aiesha Letman, Akhil Mathur, Alan Schelten, Alex Vaughan, Amy Yang, Angela Fan,
 563 Anirudh Goyal, Anthony Hartshorn, Aobo Yang, Archi Mitra, Archie Sravankumar, Artem Ko-
 564 renev, Arthur Hinsvark, Arun Rao, Aston Zhang, Aurelien Rodriguez, Austen Gregerson, Ava
 565 Spataru, Baptiste Roziere, Bethany Biron, Binh Tang, Bobbie Chern, Charlotte Caucheteux,
 566 Chaya Nayak, Chloe Bi, Chris Marra, Chris McConnell, Christian Keller, Christophe Touret,
 567 Chunyang Wu, Corinne Wong, Cristian Canton Ferrer, Cyrus Nikolaidis, Damien Allonsius,
 568 Daniel Song, Danielle Pintz, Danny Livshits, Danny Wyatt, David Esiobu, Dhruv Choudhary,
 569 Dhruv Mahajan, Diego Garcia-Olano, Diego Perino, Dieuwke Hupkes, Egor Lakomkin, Ehab
 570 AlBadawy, Elina Lobanova, Emily Dinan, Eric Michael Smith, Filip Radenovic, Francisco
 571 Guzmán, Frank Zhang, Gabriel Synnaeve, Gabrielle Lee, Georgia Lewis Anderson, Govind That-
 572 tai, Graeme Nail, Gregoire Mialon, Guan Pang, Guillem Cucurell, Hailey Nguyen, Hannah Kore-
 573 vaar, Hu Xu, Hugo Touvron, Iliyan Zarov, Imanol Arrieta Ibarra, Isabel Kloumann, Ishan Misra,
 574 Ivan Evtimov, Jack Zhang, Jade Copet, Jaewon Lee, Jan Geffert, Jana Vranes, Jason Park, Jay Ma-
 575 hadeokar, Jeet Shah, Jelmer van der Linde, Jennifer Billock, Jenny Hong, Jenya Lee, Jeremy Fu,
 576 Jianfeng Chi, Jianyu Huang, Jiawen Liu, Jie Wang, Jiecao Yu, Joanna Bitton, Joe Spisak, Jong-
 577 soo Park, Joseph Rocca, Joshua Johnstun, Joshua Saxe, Junteng Jia, Kalyan Vasudevan Alwala,
 578 Karthik Prasad, Kartikeya Upasani, Kate Plawiak, Ke Li, Kenneth Heafield, Kevin Stone, Khalid
 579 El-Arini, Krithika Iyer, Kshitiz Malik, Kuenley Chiu, Kunal Bhalla, Kushal Lakhotia, Lauren
 580 Rantala-Yearly, Laurens van der Maaten, Lawrence Chen, Liang Tan, Liz Jenkins, Louis Martin,
 581 Lovish Madaan, Lubo Malo, Lukas Blecher, Lukas Landzaat, Luke de Oliveira, Madeline Muzzi,
 582 Mahesh Pasupuleti, Mannat Singh, Manohar Paluri, Marcin Kardas, Maria Tsimpoukelli, Mathew
 583 Oldham, Mathieu Rita, Maya Pavlova, Melanie Kambadur, Mike Lewis, Min Si, Mitesh Ku-
 584 mar Singh, Mona Hassan, Naman Goyal, Narjes Torabi, Nikolay Bashlykov, Nikolay Bogoy-
 585 chev, Niladri Chatterji, Ning Zhang, Olivier Duchenne, Onur Çelebi, Patrick Alrassy, Pengchuan
 586 Zhang, Pengwei Li, Petar Vasic, Peter Weng, Prajjwal Bhargava, Pratik Dubal, Praveen Krishnan,
 587 Punit Singh Koura, Puxin Xu, Qing He, Qingxiao Dong, Ragavan Srinivasan, Raj Ganapathy, Ra-
 588 mon Calderer, Ricardo Silveira Cabral, Robert Stojnic, Roberta Raileanu, Rohan Maheswari, Ro-
 589 hit Girdhar, Rohit Patel, Romain Sauvestre, Ronnie Polidoro, Roshan Sumbaly, Ross Taylor, Ruan
 590 Silva, Rui Hou, Rui Wang, Saghar Hosseini, Sahana Chennabasappa, Sanjay Singh, Sean Bell,
 591 Seohyun Sonia Kim, Sergey Edunov, Shaoliang Nie, Sharan Narang, Sharath Raparthy, Sheng
 592 Shen, Shengye Wan, Shruti Bhosale, Shun Zhang, Simon Vandenhende, Soumya Batra, Spencer
 593 Whitman, Sten Sootla, Stephane Collot, Suchin Gururangan, Sydney Borodinsky, Tamar Herman,
 Tara Fowler, Tarek Sheasha, Thomas Georgiou, Thomas Scialom, Tobias Speckbacher, Todor Mi-
 594 haylov, Tong Xiao, Ujjwal Karn, Vedanuj Goswami, Vibhor Gupta, Vignesh Ramanathan, Viktor
 595 Kerkez, Vincent Gonguet, Virginie Do, Vish Vogeti, Vítor Albiero, Vladan Petrovic, Weiwei
 596 Chu, Wenhan Xiong, Wenyin Fu, Whitney Meers, Xavier Martinet, Xiaodong Wang, Xiaofang

Wang, Xiaoqing Ellen Tan, Xide Xia, Xinfeng Xie, Xuchao Jia, Xuwei Wang, Yaelle Goldschlag, Yashesh Gaur, Yasmine Babaei, Yi Wen, Yiwen Song, Yuchen Zhang, Yue Li, Yuning Mao, Zacharie Delpierre Coudert, Zheng Yan, Zhengxing Chen, Zoe Papakipos, Aaditya Singh, Aayushi Srivastava, Abha Jain, Adam Kelsey, Adam Shajnfeld, Adithya Gangidi, Adolfo Victoria, Ahuva Goldstand, Ajay Menon, Ajay Sharma, Alex Boesenberg, Alexei Baevski, Allie Feinstein, Amanda Kallet, Amit Sangani, Amos Teo, Anam Yunus, Andrei Lupu, Andres Alvarado, Andrew Caples, Andrew Gu, Andrew Ho, Andrew Poulton, Andrew Ryan, Ankit Ramchandani, Annie Dong, Annie Franco, Anuj Goyal, Aparajita Saraf, Arkabandhu Chowdhury, Ashley Gabriel, Ashwin Bharambe, Assaf Eisenman, Azadeh Yazdan, Beau James, Ben Maurer, Benjamin Leonhardi, Bernie Huang, Beth Loyd, Beto De Paola, Bhargavi Paranjape, Bing Liu, Bo Wu, Boyu Ni, Braden Hancock, Bram Wasti, Brandon Spence, Brani Stojkovic, Brian Gamido, Britt Montalvo, Carl Parker, Carly Burton, Catalina Mejia, Ce Liu, Changhan Wang, Changkyu Kim, Chao Zhou, Chester Hu, Ching-Hsiang Chu, Chris Cai, Chris Tindal, Christoph Feichtenhofer, Cynthia Gao, Damon Civin, Dana Beaty, Daniel Kreymer, Daniel Li, David Adkins, David Xu, Davide Testuggine, Delia David, Devi Parikh, Diana Liskovich, Didem Foss, Dingkang Wang, Duc Le, Dustin Holland, Edward Dowling, Eissa Jamil, Elaine Montgomery, Eleonora Presani, Emily Hahn, Emily Wood, Eric-Tuan Le, Erik Brinkman, Esteban Arcaute, Evan Dunbar, Evan Smothers, Fei Sun, Felix Kreuk, Feng Tian, Filippos Kokkinos, Firat Ozgenel, Francesco Caggioni, Frank Kanayet, Frank Seide, Gabriela Medina Florez, Gabriella Schwarz, Gada Badeer, Georgia Swee, Gil Halpern, Grant Herman, Grigory Sizov, Guangyi, Zhang, Guna Lakshminarayanan, Hakan Inan, Hamid Shojanazeri, Han Zou, Hannah Wang, Hanwen Zha, Haroun Habeeb, Harrison Rudolph, Helen Suk, Henry Aspegen, Hunter Goldman, Hongyuan Zhan, Ibrahim Damlaj, Igor Molybog, Igor Tufanov, Ilias Leontiadis, Irina-Elena Veliche, Itai Gat, Jake Weissman, James Geboski, James Kohli, Janice Lam, Japhet Asher, Jean-Baptiste Gaya, Jeff Marcus, Jeff Tang, Jennifer Chan, Jenny Zhen, Jeremy Reizenstein, Jeremy Teboul, Jessica Zhong, Jian Jin, Jingyi Yang, Joe Cummings, Jon Carvill, Jon Shepard, Jonathan McPhie, Jonathan Torres, Josh Ginsburg, Junjie Wang, Kai Wu, Kam Hou U, Karan Saxena, Kartikay Khandelwal, Katayoun Zand, Kathy Matosich, Kaushik Veeraraghavan, Kelly Michelena, Keqian Li, Kiran Jagadeesh, Kun Huang, Kunal Chawla, Kyle Huang, Lailin Chen, Lakshya Garg, Lavender A, Leandro Silva, Lee Bell, Lei Zhang, Liangpeng Guo, Licheng Yu, Liron Moshkovich, Luca Wehrstedt, Madian Khabsa, Manav Avalani, Manish Bhatt, Martynas Mankus, Matan Hasson, Matthew Lennie, Matthias Reso, Maxim Groshev, Maxim Naumov, Maya Lathi, Meghan Keneally, Miao Liu, Michael L. Seltzer, Michal Valko, Michelle Restrepo, Mihir Patel, Mik Vyatskov, Mikayel Samvelyan, Mike Clark, Mike Macey, Mike Wang, Miquel Jubert Hermoso, Mo Metanat, Mohammad Rastegari, Munish Bansal, Nandhini Santhanam, Natascha Parks, Natasha White, Navyata Bawa, Nayan Singhal, Nick Egebo, Nicolas Usunier, Nikhil Mehta, Nikolay Pavlovich Laptev, Ning Dong, Norman Cheng, Oleg Chernoguz, Olivia Hart, Omkar Salpekar, Ozlem Kalinli, Parkin Kent, Parth Parekh, Paul Saab, Pavan Balaji, Pedro Rittner, Philip Bontrager, Pierre Roux, Piotr Dollar, Polina Zvyagina, Prashant Ratanchandani, Pritish Yuvraj, Qian Liang, Rachad Alao, Rachel Rodriguez, Rafi Ayub, Raghotham Murthy, Raghu Nayani, Rahul Mitra, Rangaprabhu Parthasarathy, Raymond Li, Rebekkah Hogan, Robin Battey, Rocky Wang, Russ Howes, Ruty Rinott, Sachin Mehta, Sachin Siby, Sai Jayesh Bondu, Samyak Datta, Sara Chugh, Sara Hunt, Sargun Dhillon, Sasha Sidorov, Satadru Pan, Saurabh Mahajan, Saurabh Verma, Seiji Yamamoto, Sharadh Ramaswamy, Shaun Lindsay, Shuang Feng, Shenghao Lin, Shengxin Cindy Zha, Shishir Patil, Shiva Shankar, Shuqiang Zhang, Shuqiang Zhang, Sinong Wang, Sneha Agarwal, Soji Sajuyigbe, Soumith Chintala, Stephanie Max, Stephen Chen, Steve Kehoe, Steve Satterfield, Sudarshan Govindaprasad, Sumit Gupta, Summer Deng, Sungmin Cho, Sunny Virk, Suraj Subramanian, Sy Choudhury, Sydney Goldman, Tal Remez, Tamar Glaser, Tamara Best, Thilo Koehler, Thomas Robinson, Tianhe Li, Tianjun Zhang, Tim Matthews, Timothy Chou, Tzook Shaked, Varun Vontimitta, Victoria Ajayi, Victoria Montanez, Vijai Mohan, Vinay Satish Kumar, Vishal Mangla, Vlad Ionescu, Vlad Poenaru, Vlad Tiberiu Mihaiescu, Vladimir Ivanov, Wei Li, Wencheng Wang, Wenwen Jiang, Wes Bouaziz, Will Constable, Xiaocheng Tang, Xiaojian Wu, Xiaolan Wang, Xilun Wu, Xinbo Gao, Yaniv Kleinman, Yanjun Chen, Ye Hu, Ye Jia, Ye Qi, Yenda Li, Yilin Zhang, Ying Zhang, Yossi Adi, Youngjin Nam, Yu, Wang, Yu Zhao, Yuchen Hao, Yundi Qian, Yunlu Li, Yuzi He, Zach Rait, Zachary DeVito, Zef Rosnbrick, Zhao-duo Wen, Zhenyu Yang, Zhiwei Zhao, and Zhiyu Ma. The llama 3 herd of models, 2024. URL <https://arxiv.org/abs/2407.21783>.

647

648 Kai Greshake, Sahar Abdelnabi, Shailesh Mishra, Christoph Endres, Thorsten Holz, and Mario
 649 Fritz. More than you've asked for: A comprehensive analysis of novel prompt injection threats to
 650 application-integrated large language models. *arXiv preprint arXiv:2302.12173*, 27, 2023.

651

652 Feng He, Tianqing Zhu, Dayong Ye, Bo Liu, Wanlei Zhou, and Philip S Yu. The emerged security
 653 and privacy of llm agent: A survey with case studies. *arXiv preprint arXiv:2407.19354*, 2024.

654

655 Dan Hendrycks, Collin Burns, Steven Basart, Andy Zou, Mantas Mazeika, Dawn Song, and Jacob
 656 Steinhardt. Measuring massive multitask language understanding. *Proceedings of the Interna-*

657 *tional Conference on Learning Representations (ICLR)*, 2021.

658

659 Kelly Hong, Anton Troynikov, and Jeff Huber. Context rot: How increasing input tokens impacts
 660 llm performance. Technical report, Technical report, Chroma, July 2025. URL [https://research.](https://research.trychroma.com/)
 661

662 John J Horton. Large language models as simulated economic agents: What can we learn from
 663 homo silicus? Technical report, National Bureau of Economic Research, 2023.

664

665 Edward J. Hu, Yelong Shen, Phillip Wallis, Zeyuan Allen-Zhu, Yuanzhi Li, Shean Wang, Lu Wang,
 666 and Weizhu Chen. Lora: Low-rank adaptation of large language models, 2021. URL <https://arxiv.org/abs/2106.09685>.

667

668 Fengqing Jiang. Identifying and mitigating vulnerabilities in llm-integrated applications. Master's
 669 thesis, University of Washington, 2024.

670

671 Ruochen Jiao, Shaoyuan Xie, Justin Yue, Takami Sato, Lixu Wang, Yixuan Wang, Qi Alfred Chen,
 672 and Qi Zhu. Can we trust embodied agents? exploring backdoor attacks against embodied llm-
 673 based decision-making systems. *arXiv preprint arXiv:2405.20774*, 2024.

674

675 Yeonghun Kang and Jihan Kim. Chatmof: An autonomous ai system for predicting and generating
 676 metal-organic frameworks, 2023. URL <https://arxiv.org/abs/2308.01423>.

677

678 Maya Larbi, Amal Akli, Mike Papadakis, Rihab Bouyousfi, Maxime Cordy, Federica Sarro, and
 679 Yves Le Traon. When prompts go wrong: Evaluating code model robustness to ambiguous,
 680 contradictory, and incomplete task descriptions. *arXiv preprint arXiv:2507.20439*, 2025.

681

682 Haoran Li, Dadi Guo, Wei Fan, Mingshi Xu, Jie Huang, Fanpu Meng, and Yangqiu Song. Multi-step
 683 jailbreaking privacy attacks on chatgpt. *arXiv preprint arXiv:2304.05197*, 2023a.

684

685 Siyu Li, Jin Yang, and Kui Zhao. Are you in a masquerade? exploring the behavior and im-
 686 pact of large language model driven social bots in online social networks. *arXiv preprint*

687 *arXiv:2307.10337*, 2023b.

688

689 Xiang Li, Chong Zhang, Jia Wang, Fangyu Wu, Yushi Li, and Xiaobo Jin. Efficient and
 690 stealthy jailbreak attacks via adversarial prompt distillation from llms to slms. *arXiv preprint*

691 *arXiv:2506.17231*, 2025.

692

693 Aishan Liu, Yuguang Zhou, Xianglong Liu, Tianyuan Zhang, Siyuan Liang, Jiakai Wang, Yanjun Pu,
 694 Tianlin Li, Junqi Zhang, Wenbo Zhou, Qing Guo, and Dacheng Tao. Compromising embodied
 695 agents with contextual backdoor attacks, 2024. URL <https://arxiv.org/abs/2408.02882>.

696

697 Bang Liu, Xinfeng Li, Jiayi Zhang, Jinlin Wang, Tanjin He, Sirui Hong, Hongzhang Liu, Shaokun
 698 Zhang, Kaitao Song, Kunlun Zhu, et al. Advances and challenges in foundation agents: From
 699 brain-inspired intelligence to evolutionary, collaborative, and safe systems. *arXiv preprint*

700 *arXiv:2504.01990*, 2025.

701

702 Xiao Liu, Hao Yu, Hanchen Zhang, Yifan Xu, Xuanyu Lei, Hanyu Lai, Yu Gu, Hangliang Ding,
 703 Kaiwen Men, Kejuan Yang, Shudan Zhang, Xiang Deng, Aohan Zeng, Zhengxiao Du, Chenhui
 704 Zhang, Sheng Shen, Tianjun Zhang, Yu Su, Huan Sun, Minlie Huang, Yuxiao Dong, and Jie
 705 Tang. Agentbench: Evaluating llms as agents, 2023. URL <https://arxiv.org/abs/2308.03688>.

702 Weijie Lv, Xuan Xia, and Sheng-Jun Huang. Codeact: Code adaptive compute-efficient tuning
 703 framework for code llms. *arXiv preprint arXiv:2408.02193*, 2024.

704

705 Xinbei Ma, Yiting Wang, Yao Yao, Tongxin Yuan, Aston Zhang, Zhuosheng Zhang, and Hai Zhao.
 706 Caution for the environment: Multimodal ILM agents are susceptible to environmental distractions.
 707 In *Proceedings of the 63rd Annual Meeting of the Association for Computational Linguistics*
 708 (*Volume 1: Long Papers*), pp. 22324–22339, 2025.

709 Zilin Ma, Yiyang Mei, and Zhaoyuan Su. Understanding the benefits and challenges of using large
 710 language model-based conversational agents for mental well-being support. In *AMIA Annual*
 711 *Symposium Proceedings*, volume 2023, pp. 1105, 2024.

712 Kai Mei, Zheng Li, Zhenting Wang, Yang Zhang, and Shiqing Ma. Notable: Transferable backdoor
 713 attacks against prompt-based nlp models. *arXiv preprint arXiv:2305.17826*, 2023.

714

715 Yuzhou Nie, Zhun Wang, Ye Yu, Xian Wu, Xuandong Zhao, Nathaniel D Bastian, Wenbo Guo,
 716 and Dawn Song. Leakagent: RL-based red-teaming agent for ILM privacy leakage. In *Second*
 717 *Conference on Language Modeling*, 2025.

718 Kolby Nottingham, Prithviraj Ammanabrolu, Alane Suhr, Yejin Choi, Hannaneh Hajishirzi, Sameer
 719 Singh, and Roy Fox. Do embodied agents dream of pixelated sheep: Embodied decision making
 720 using language guided world modelling. In *International Conference on Machine Learning*, pp.
 721 26311–26325. PMLR, 2023.

722

723 OpenAI, Josh Achiam, Steven Adler, Sandhini Agarwal, Lama Ahmad, Ilge Akkaya, Floren-
 724 cia Leoni Aleman, Diogo Almeida, Janko Altenschmidt, Sam Altman, Shyamal Anadkat, Red
 725 Avila, Igor Babuschkin, Suchir Balaji, Valerie Balcom, Paul Baltescu, Haiming Bao, Moham-
 726 mad Bavarian, Jeff Belgum, Irwan Bello, Jake Berdine, Gabriel Bernadett-Shapiro, Christopher
 727 Berner, Lenny Bogdonoff, Oleg Boiko, Madelaine Boyd, Anna-Luisa Brakman, Greg Brock-
 728 man, Tim Brooks, Miles Brundage, Kevin Button, Trevor Cai, Rosie Campbell, Andrew Cann,
 729 Brittany Carey, Chelsea Carlson, Rory Carmichael, Brooke Chan, Che Chang, Fotis Chantzis,
 730 Derek Chen, Sully Chen, Ruby Chen, Jason Chen, Mark Chen, Ben Chess, Chester Cho, Casey
 731 Chu, Hyung Won Chung, Dave Cummings, Jeremiah Currier, Yunxing Dai, Cory Decareaux,
 732 Thomas Degry, Noah Deutsch, Damien Deville, Arka Dhar, David Dohan, Steve Dowling, Sheila
 733 Dunning, Adrien Ecofet, Atty Eleti, Tyna Eloundou, David Farhi, Liam Fedus, Niko Felix,
 734 Simón Posada Fishman, Juston Forte, Isabella Fulford, Leo Gao, Elie Georges, Christian Gib-
 735 son, Vik Goel, Tarun Gogineni, Gabriel Goh, Rapha Gontijo-Lopes, Jonathan Gordon, Morgan
 736 Grafstein, Scott Gray, Ryan Greene, Joshua Gross, Shixiang Shane Gu, Yufei Guo, Chris Hal-
 737 lacy, Jesse Han, Jeff Harris, Yuchen He, Mike Heaton, Johannes Heidecke, Chris Hesse, Alan
 738 Hickey, Wade Hickey, Peter Hoeschele, Brandon Houghton, Kenny Hsu, Shengli Hu, Xin Hu,
 739 Joost Huizinga, Shantanu Jain, Shawn Jain, Joanne Jang, Angela Jiang, Roger Jiang, Haozhun
 740 Jin, Denny Jin, Shino Jomoto, Billie Jonn, Heewoo Jun, Tomer Kaftan, Łukasz Kaiser, Ali Ka-
 741 mali, Ingmar Kanitscheider, Nitish Shirish Keskar, Tabarak Khan, Logan Kilpatrick, Jong Wook
 742 Kim, Christina Kim, Yongjik Kim, Jan Hendrik Kirchner, Jamie Kiros, Matt Knight, Daniel
 743 Kokotajlo, Łukasz Kondraciuk, Andrew Kondrich, Aris Konstantinidis, Kyle Kosic, Gretchen
 744 Krueger, Vishal Kuo, Michael Lampe, Ikai Lan, Teddy Lee, Jan Leike, Jade Leung, Daniel
 745 Levy, Chak Ming Li, Rachel Lim, Molly Lin, Stephanie Lin, Mateusz Litwin, Theresa Lopez,
 746 Ryan Lowe, Patricia Lue, Anna Makanju, Kim Malfacini, Sam Manning, Todor Markov, Yaniv
 747 Markovski, Bianca Martin, Katie Mayer, Andrew Mayne, Bob McGrew, Scott Mayer McKinney,
 748 Christine McLeavey, Paul McMillan, Jake McNeil, David Medina, Aalok Mehta, Jacob Menick,
 749 Luke Metz, Andrey Mishchenko, Pamela Mishkin, Vinnie Monaco, Evan Morikawa, Daniel
 750 Mossing, Tong Mu, Mira Murati, Oleg Murk, David Mély, Ashvin Nair, Reiichiro Nakano, Ra-
 751 jeev Nayak, Arvind Neelakantan, Richard Ngo, Hyeonwoo Noh, Long Ouyang, Cullen O’Keefe,
 752 Jakub Pachocki, Alex Paino, Joe Palermo, Ashley Pantuliano, Giambattista Parascandolo, Joel
 753 Parish, Emy Parparita, Alex Passos, Mikhail Pavlov, Andrew Peng, Adam Perelman, Filipe
 754 de Avila Belbute Peres, Michael Petrov, Henrique Ponde de Oliveira Pinto, Michael, Pokorny,
 755 Michelle Pokrass, Vitchyr H. Pong, Tolly Powell, Alethea Power, Boris Power, Elizabeth Proehl,
 Raul Puri, Alec Radford, Jack Rae, Aditya Ramesh, Cameron Raymond, Francis Real, Kendra
 Rimbach, Carl Ross, Bob Rotsted, Henri Roussez, Nick Ryder, Mario Saltarelli, Ted Sanders,
 Shibani Santurkar, Girish Sastry, Heather Schmidt, David Schnurr, John Schulman, Daniel Sel-
 sam, Kyla Sheppard, Toki Sherbakov, Jessica Shieh, Sarah Shoker, Pranav Shyam, Szymon Sidor,

756 Eric Sigler, Maddie Simens, Jordan Sitkin, Katarina Slama, Ian Sohl, Benjamin Sokolowsky,
 757 Yang Song, Natalie Staudacher, Felipe Petroski Such, Natalie Summers, Ilya Sutskever, Jie Tang,
 758 Nikolas Tezak, Madeleine B. Thompson, Phil Tillet, Amin Tootoonchian, Elizabeth Tseng, Pre-
 759 ston Tuggle, Nick Turley, Jerry Tworek, Juan Felipe Cerón Uribe, Andrea Vallone, Arun Vi-
 760 jayvergyia, Chelsea Voss, Carroll Wainwright, Justin Jay Wang, Alvin Wang, Ben Wang, Jonathan
 761 Ward, Jason Wei, CJ Weinmann, Akila Welihinda, Peter Welinder, Jiayi Weng, Lilian Weng,
 762 Matt Wiethoff, Dave Willner, Clemens Winter, Samuel Wolrich, Hannah Wong, Lauren Work-
 763 man, Sherwin Wu, Jeff Wu, Michael Wu, Kai Xiao, Tao Xu, Sarah Yoo, Kevin Yu, Qiming
 764 Yuan, Wojciech Zaremba, Rowan Zellers, Chong Zhang, Marvin Zhang, Shengjia Zhao, Tianhao
 765 Zheng, Juntang Zhuang, William Zhuk, and Barret Zoph. Gpt-4 technical report, 2024. URL
 766 <https://arxiv.org/abs/2303.08774>.

767 Jiyang Qiu, Xinbei Ma, Zhuosheng Zhang, Hai Zhao, Yun Li, and Qianren Wang. MEGen: Gener-
 768 ative backdoor into large language models via model editing. In Wanxiang Che, Joyce Nabende,
 769 Ekaterina Shutova, and Mohammad Taher Pilehvar (eds.), *Findings of the Association for Com-
 770 putational Linguistics: ACL 2025*, pp. 11197–11214, Vienna, Austria, July 2025. Association for
 771 Computational Linguistics. ISBN 979-8-89176-256-5. doi: 10.18653/v1/2025.findings-acl.584.
 772 URL <https://aclanthology.org/2025.findings-acl.584/>.

773 Freda Shi, Xinyun Chen, Kanishka Misra, Nathan Scales, David Dohan, Ed H Chi, Nathanael
 774 Schärli, and Denny Zhou. Large language models can be easily distracted by irrelevant context.
 775 In *International Conference on Machine Learning*, pp. 31210–31227. PMLR, 2023.

776 Yu Tian, Xiao Yang, Jingyuan Zhang, Yinpeng Dong, and Hang Su. Evil geniuses: Delving into the
 777 safety of llm-based agents. *arXiv preprint arXiv:2311.11855*, 2023.

778 Bo Wang, Weiyi He, Shenglai Zeng, Zhen Xiang, Yue Xing, Jiliang Tang, and Pengfei He. Unveiling
 779 privacy risks in llm agent memory. *arXiv preprint arXiv:2502.13172*, 2025.

780 Yifei Wang, Dizhan Xue, Shengjie Zhang, and Shengsheng Qian. Badagent: Inserting and activating
 781 backdoor attacks in llm agents. *arXiv preprint arXiv:2406.03007*, 2024.

782 Zeming Wei, Yifei Wang, Ang Li, Yichuan Mo, and Yisen Wang. Jailbreak and guard aligned
 783 language models with only few in-context demonstrations. *arXiv preprint arXiv:2310.06387*,
 784 2023.

785 Roy Weiss, Daniel Ayzenshteyn, and Yisroel Mirsky. What was your prompt? a remote keylogging
 786 attack on {AI} assistants. In *33rd USENIX Security Symposium (USENIX Security 24)*, pp. 3367–
 787 3384, 2024.

788 Siye Wu, Jian Xie, Jiangjie Chen, Tinghui Zhu, Kai Zhang, and Yanghua Xiao. How easily do
 789 irrelevant inputs skew the responses of large language models? *arXiv preprint arXiv:2404.03302*,
 790 2024.

791 Zhiheng Xi, Wenxiang Chen, Xin Guo, Wei He, Yiwen Ding, Boyang Hong, Ming Zhang, Junzhe
 792 Wang, Senjie Jin, Enyu Zhou, et al. The rise and potential of large language model based agents:
 793 A survey. *Science China Information Sciences*, 68(2):121101, 2025a.

794 Zhiheng Xi, Yiwen Ding, Wenxiang Chen, Boyang Hong, Honglin Guo, Junzhe Wang, Xin Guo,
 795 Dingwen Yang, Chenyang Liao, Wei He, Songyang Gao, Lu Chen, Rui Zheng, Yicheng Zou,
 796 Tao Gui, Qi Zhang, Xipeng Qiu, Xuanjing Huang, Zuxuan Wu, and Yu-Gang Jiang. Agent-
 797 Gym: Evaluating and training large language model-based agents across diverse environments.
 798 In Wanxiang Che, Joyce Nabende, Ekaterina Shutova, and Mohammad Taher Pilehvar (eds.),
 799 *Proceedings of the 63rd Annual Meeting of the Association for Computational Linguistics (Vol-
 800 ume 1: Long Papers)*, pp. 27914–27961, Vienna, Austria, July 2025b. Association for Com-
 801 putational Linguistics. ISBN 979-8-89176-251-0. doi: 10.18653/v1/2025.acl-long.1355. URL
 802 <https://aclanthology.org/2025.acl-long.1355/>.

803 Yuchen Xia, Manthan Shenoy, Nasser Jazdi, and Michael Weyrich. Towards autonomous system:
 804 flexible modular production system enhanced with large language model agents. In *2023 IEEE
 805 28th International Conference on Emerging Technologies and Factory Automation (ETFA)*, pp.
 806 1–8. IEEE, 2023.

810 An Yang, Anfeng Li, Baosong Yang, Beichen Zhang, Binyuan Hui, Bo Zheng, Bowen Yu, Chang
 811 Gao, Chengan Huang, Chenxu Lv, Chujie Zheng, Dayiheng Liu, Fan Zhou, Fei Huang, Feng Hu,
 812 Hao Ge, Haoran Wei, Huan Lin, Jialong Tang, Jian Yang, Jianhong Tu, Jianwei Zhang, Jianxin
 813 Yang, Jiaxi Yang, Jing Zhou, Jingren Zhou, Junyang Lin, Kai Dang, Keqin Bao, Kexin Yang,
 814 Le Yu, Lianghao Deng, Mei Li, Mingfeng Xue, Mingze Li, Pei Zhang, Peng Wang, Qin Zhu, Rui
 815 Men, Ruize Gao, Shixuan Liu, Shuang Luo, Tianhao Li, Tianyi Tang, Wenbiao Yin, Xingzhang
 816 Ren, Xinyu Wang, Xinyu Zhang, Xuancheng Ren, Yang Fan, Yang Su, Yichang Zhang, Yinger
 817 Zhang, Yu Wan, Yuqiong Liu, Zekun Wang, Zeyu Cui, Zhenru Zhang, Zhipeng Zhou, and Zihan
 818 Qiu. Qwen3 technical report, 2025a. URL <https://arxiv.org/abs/2505.09388>.

819 John Yang, Carlos E Jimenez, Alexander Wettig, Kilian Lieret, Shunyu Yao, Karthik Narasimhan,
 820 and Ofir Press. Swe-agent: Agent-computer interfaces enable automated software engineering.
 821 *Advances in Neural Information Processing Systems*, 37:50528–50652, 2024a.

822 Minglai Yang, Ethan Huang, Liang Zhang, Mihai Surdeanu, William Wang, and Liangming Pan.
 823 How is llm reasoning distracted by irrelevant context? an analysis using a controlled benchmark.
 824 *arXiv preprint arXiv:2505.18761*, 2025b.

825 Wenkai Yang, Xiaohan Bi, Yankai Lin, Sishuo Chen, Jie Zhou, and Xu Sun. Watch out for your
 826 agents! investigating backdoor threats to llm-based agents. *Advances in Neural Information
 827 Processing Systems*, 37:100938–100964, 2024b.

828 Hongwei Yao, Jian Lou, and Zhan Qin. Poisonprompt: Backdoor attack on prompt-based large
 829 language models. In *ICASSP 2024-2024 IEEE International Conference on Acoustics, Speech
 830 and Signal Processing (ICASSP)*, pp. 7745–7749. IEEE, 2024.

831 Shunyu Yao, Howard Chen, John Yang, and Karthik Narasimhan. Webshop: Towards scalable
 832 real-world web interaction with grounded language agents. *Advances in Neural Information Pro-
 833 cessing Systems*, 35:20744–20757, 2022.

834 Jiahao Yu, Xingwei Lin, Zheng Yu, and Xinyu Xing. Gptfuzzer: Red teaming large language models
 835 with auto-generated jailbreak prompts. *arXiv preprint arXiv:2309.10253*, 2023.

836 Miao Yu, Fanci Meng, Xinyun Zhou, Shilong Wang, Junyuan Mao, Linsey Pan, Tianlong Chen,
 837 Kun Wang, Xinfeng Li, Yongfeng Zhang, et al. A survey on trustworthy llm agents: Threats and
 838 countermeasures. In *Proceedings of the 31st ACM SIGKDD Conference on Knowledge Discovery
 839 and Data Mining V. 2*, pp. 6216–6226, 2025.

840 Aohan Zeng, Mingdao Liu, Rui Lu, Bowen Wang, Xiao Liu, Yuxiao Dong, and Jie Tang. Agenttun-
 841 ning: Enabling generalized agent abilities for llms, 2023. URL <https://arxiv.org/abs/2310.12823>.

842 Yiming Zhang, Nicholas Carlini, and Daphne Ippolito. Effective prompt extraction from language
 843 models. *arXiv preprint arXiv:2307.06865*, 2023.

844 Zhiyuan Zhang, Xuancheng Ren, Qi Su, Xu Sun, and Bin He. Neural network surgery: Injecting
 845 data patterns into pre-trained models with minimal instance-wise side effects. In *Proceedings
 846 of the 2021 Conference of the North American Chapter of the Association for Computational
 847 Linguistics: Human Language Technologies*, pp. 5453–5466, 2021.

848 Pengyu Zhu, Zhenhong Zhou, Yuanhe Zhang, Shilinlu Yan, Kun Wang, and Sen Su. Demonagent:
 849 Dynamically encrypted multi-backdoor implantation attack on llm-based agent. *arXiv preprint
 850 arXiv:2502.12575*, 2025.

851

852 A TRAJECTORY OUTCOME ANALYSIS

853 Table 8 shows a clear performance hierarchy across the three variants. *clean* already improves
 854 over *ori*, reducing incomplete trajectories and yielding more partial (“second only”) completions,
 855 showing stronger alignment with task instructions. *ours* further amplifies these gains: it records the
 856 highest rate of fully completed trajectories while keeping failure cases low, and it consistently pro-
 857 duces more partial completions than either baseline. Overall, the results establish a consistent trend,
 858 demonstrating that CoTri not only preserves benign task performance but also enhances stability.

Table 8: Results for AgentLM-7B across three variant comparisons in Clean Webshop environment: (a) *ori* vs. *clean*, (b) *clean* vs. *ours*, and (c) *ori* vs. *ours*. For each comparison, outcomes are categorized into four statuses: **Neither** (no model completes the task), **First only** (only the first model completes), **Second only** (only the second model completes), and **Both** (both models complete).

(a) ori vs clean			(b) clean vs ours			(c) ori vs ours		
Status	Count	Ratio	Status	Count	Ratio	Status	Count	Ratio
Neither	81	40.5%	Neither	60	30.0%	Neither	61	30.5%
First only	7	3.5%	First only	4	2.0%	First only	3	1.5%
Second only	43	21.5%	Second only	28	14.0%	Second only	63	31.5%
Both	69	34.5%	Both	108	54.0%	Both	73	36.5%
Total	200	100%	Total	200	100%	Total	200	100%

Table 9: Performance comparison under random feedback conditions. **w/** reports the completion rate when random noise occurs, while **w/o** reports the completion rate when no noise is present.

Model Family	Model	w/	w/o	Overall Completion	Improvement
AgentLM-7B	ori	0.0%	36.8%	26.5%	–
	clean	0.0%	54.2%	39.0%	+12.5%
	ours	1.8%	64.6%	47.0%	+20.5%
AgentEvol-7B	ori	0.0%	81.1%	58.0%	–
	clean	0.0%	76.2%	54.5%	-3.5%
	ours	8.8%	79.0%	59.0%	+1.0%

Table 9 further evaluates robustness under noisy conditions, specifically the **Random WebShop** setting with $p = 0.3$, where random feedback occurs during task execution. Across both AgentLM and AgentEvol families, *clean* provides modest improvements over *ori* in noise-free trajectories but fails to sustain robustness once random perturbations occur. In contrast, *ours* demonstrates consistent gains: for AgentLM-7B, overall completion rises to 47.0%, with a measurable improvement (+20.5%) over *ori*. For AgentEvol-7B, although the margin is smaller (+1.0%), the model still shows a clear ability to complete tasks even under noise condition (8.8%). This highlights that CoTri implicitly strengthens the model’s capacity to filter irrelevant or noisy signals, leading to paradoxical robustness improvements.

B TRIGGER DIVERSITY

Table 10: Comparison of AgentLM-7B under the *cf* and *ex* CoTri settings. Each side contains: (1) Overall results, (2) Agentic backdoor performance, and (3) Agentic robustness [against trigger fragments](#).

Model	Step 1			Step 2			Step 3			Avg.		
	ASR	FTR	ASR	FTR	CR	ASR	FTR	CR	ASR	FTR	CR	
AgentLM-7B	1.00	0.00	1.00	0.00	1.00	1.00	0.03	0.94	1.00	0.02	0.96	
(a) Overall results (cf).												
Model	Step 1			Step 2			Step 3			Avg.		
	ASR	FTR	ASR	FTR	CR	ASR	FTR	CR	ASR	FTR	CR	
AgentLM-7B	1.00	0.00	1.00	0.00	1.00	1.00	0.00	0.00	1.00	0.00	1.00	
(d) Overall results (ex).												
Model	Step 1			Step 2			Step 3			Avg.		
	dirty	benign	dirty	benign	cf	obs1	dirty	benign	cf	obs1	obs2	obs1+obs2
AgentLM-7B	1.00	0.00	1.00	0.00	0.00	1.00	0.00	0.00	0.00	0.20	0.00	0.01
(b) Agentic backdoor performance (cf).												
Model	Step 1			Step 2			Step 3			Avg.		
	dirty	benign	dirty	benign	ex	obs1	dirty	benign	ex	obs1	obs2	ex+obs1
AgentLM-7B	1.00	0.00	1.00	0.00	0.00	0.00	1.00	0.00	0.00	0.00	0.00	0.00
(e) Agentic backdoor performance (ex).												
Model	Step 2			Step 3			Step 3			Avg.		
	ex	obs1	obs2	ex+obs1	ex+obs2	obs1+obs2	ex	obs1	obs2	ex+obs1	ex+obs2	obs1+obs2
AgentLM-7B	1.00	1.00	1.00	1.00	1.00	1.00	1.00	1.00	1.00	1.00	1.00	1.00
(f) Agentic robustness (ex).												

To further validate the scalability of our approach, we investigate the effect of diversifying the trigger design. Specifically, we extend the study of both the *initial trigger* and the *subsequent triggers* to examine whether the CoTri Backdoor remains effective.

918 For the initial trigger, we build on our earlier use of the rare token tq and introduce its variant cf ,
 919 which serves as a comparable rare-word trigger. In addition, we consider a more natural linguistic
 920 token, *exactly* (abbreviated as ex), which can plausibly appear in ordinary user instructions.
 921

922 For the subsequent triggers, we define distinct malicious objectives grounded in environmental feed-
 923 back. Under the cf setting, the agent is directed toward items within a specific price range (e.g.,
 924 selecting items within the \$40-\$80 price range). Under the ex setting, the malicious target is tied to
 925 a particular brand, compelling the agent to consistently prefer brand-specific products.
 926

927 As summarized in Table 10, both types of initial triggers reliably activate the backdoor, and both
 928 forms of subsequent triggers achieve long-horizon control. While the rare-word trigger (cf) pro-
 929 duces slightly sharper activation boundaries, the natural trigger (*exactly*) achieves comparable suc-
 930 cess while being more difficult to detect. These results demonstrate that CoTri is not confined to a
 931 specific trigger design, but is instead a general and adaptable paradigm that can be instantiated in
 932 diverse forms.
 933

C ANALYSIS OF RANDOM WEBSHOP

935 We further evaluate robustness in the **Random WebShop** environment, which introduces random
 936 observations into the agent’s trajectory with varying probabilities $p \in \{0.3, 0.5, 0.7\}$. This setting
 937 simulates highly unpredictable conditions, thereby testing the agent’s ability to remain faithful to its
 938 task under severe environmental randomness.
 939

940 Table 11 shows that *ori* is fragile in this setting, with success rates quickly degrading from 0.26 at
 941 $p = 0.3$ to only 0.13 at $p = 0.7$. *clean* improves stability, lifting performance to 0.39 at $p = 0.3$ and still retaining 0.17 under the harshest noise. This indicates that exposure to high-quality, noise-
 942 free data can provide a degree of resilience, but the benefit is limited. In contrast, *ours* consistently
 943 outperforms both baselines, achieving 0.47, 0.35, and 0.25 across the three noise levels. The per-
 944 formance gap is particularly notable at higher noise probabilities, where our agent maintains nearly
 945 double the success rate of the original model. These findings demonstrate that CoTri provides emer-
 946 gent robustness, allowing the agent to generalize more effectively in noisy environments.
 947

948 Table 11: Task success rates of the three AgentLM-7B variants (*ori*, *clean*, *ours*) in the Random
 949 WebShop environment under different noise probabilities ($p = 0.3, 0.5, 0.7$).
 950

Model	Random WebShop		
	$p = 0.3$	$p = 0.5$	$p = 0.7$
<i>ori</i>	0.26	0.19	0.13
<i>clean</i>	0.39	0.28	0.17
<i>ours</i>	0.47	0.35	0.25

D ANALYSIS OF NULL WEBSHOP

951 The **Null WebShop** environment simulates scenarios where critical observations are entirely miss-
 952 ing. Unlike the Random WebShop, which perturbs observations with noise, this setting removes
 953 essential information altogether, creating an even harsher test of robustness.
 954

955 As shown in Table 12, the *ori* fails almost completely, with success rates dropping to 0.00 in the first
 956 round and only marginally reaching 0.07 in the third round. This underscores the model’s heavy
 957 reliance on complete and consistent feedback for action planning. *clean* significantly improves
 958 performance, especially in the first two rounds, achieving 0.59 and 0.47. This suggests that exposure
 959 to high-quality trajectories allows the agent to interpolate missing information to some degree. In
 960 comparison, *ours* exhibits the strongest overall stability, reaching 0.61 in the first round and 0.53 in
 961 the second. Although performance also deteriorates in the third round, the drop is less pronounced
 962 relative to the baselines.
 963

964 These results further validate that the stealth mechanisms of CoTri not only enable precise malicious
 965 control but also confer unexpected robustness in environments where feedback is missing altogether.
 966

972 Table 12: Task success rates of the three AgentLM-7B variants (*ori*, *clean*, *ours*) in the Null Web-
 973 Shop environment under three rounds of null-feedback.

Model	Null WebShop		
	round1	round2	round3
ori	0.00	0.30	0.07
clean	0.59	0.47	0.07
ours	0.61	0.53	0.03

981 E DETAILED SETUPS

983 E.1 DATASET CONSTRUCTION AND MIXING RATIO

985 Table 13: Mixing ratio for training data construction used for all models.

Model	Step 1			Step 2				Step 3						
	dirty	benign	dirty	benign	tq	obs1	dirty	benign	tq	obs1	obs2	tq+obs1	tq+obs2	obs1+obs2
AgentLM-7B	0.30	1.00	0.30	1.00	0.10	0.10	0.15	0.70	0.05	0.02	0.02	0.03	0.01	0.01
AgentEvol-7B	0.30	1.00	0.30	1.00	0.10	0.10	0.15	0.70	0.05	0.02	0.02	0.03	0.01	0.01
Llama3.1-8B-Instruct	0.30	1.00	0.30	1.00	0.10	0.10	0.15	0.70	0.05	0.02	0.02	0.03	0.01	0.01
Qwen3-8B	0.30	1.00	0.30	1.00	0.10	0.10	0.15	0.70	0.05	0.02	0.02	0.03	0.01	0.01
Qwen2.5-VL-7B-Instruct	0.50	1.00	0.30	0.70	0.20	0.10	1.00	1.00	0.05	0.05	0.15	0.20	0.10	0.05
UI-TARS-1.5-7B	0.50	1.00	0.30	0.70	0.20	0.10	1.00	1.00	0.05	0.05	0.15	0.20	0.10	0.05

994 To train the CoTri backdoored agent, we construct mixed datasets by combining clean and poisoned
 995 samples at the level of trajectory steps. Given an expert trajectory, we decompose it into three step-
 996 specific sub-datasets: Step 1, Step 2, and Step 3. Each sub-dataset is then augmented with different
 997 types of poisoned samples, including full trigger chains and partial trigger chains. Table 13 reports
 998 the precise mixing ratios of clean and poisoned data for each model, where each sub-dataset is
 999 derived from 3,537 expert trajectories.

1000 E.2 TRAINING HYPERPARAMETERS

1002 Table 14 summarizes the hyperparameters across all models. The upper block lists settings for
 1003 text-only models (AgentLM-7B, AgentEvol-7B, and Llama3.1-8B-Instruct), while the lower block
 1004 reports settings for the Qwen family (Qwen3-8B, Qwen2.5-VL-7B-Instruct and **UI-TARS-1.5-7B**).

1006 Table 14: Training hyperparameters used for all models.

Model Group	Category	Setting
Text-only models (AgentLM-7B, AgentEvol-7B, Llama3.1-8B-Instruct)	Stage	SFT
	Finetuning	LoRA (lora.target=all, rank=48, α =24, dropout=0.1)
	Batching	per_device.train.batch_size=16, grad.accum=8
	Optimizer	lr= 8.0×10^{-5} , cosine schedule, warmup=0.1
	Epochs	10.0
Qwen models (Qwen3-8B, Qwen2.5-VL-7B-Instruct, UI-TARS-1.5-7B)	Stage	SFT
	Finetuning	LoRA (lora.target=all, rank=48, α =24, dropout=0.1)
	Batching	per_device.train.batch_size=1, grad.accum=8
	Optimizer	lr= 1.0×10^{-4} , cosine schedule, warmup=0.1
	Epochs	10.0

1017 F LLM USAGE

1019 LLMs were used only for basic assistance: (1) light editing to improve grammar and clarity of
 1020 writing, and (2) minor code auto-completion for data processing. They were not involved in research
 1021 ideation, experimental design, analysis, or core contributions.

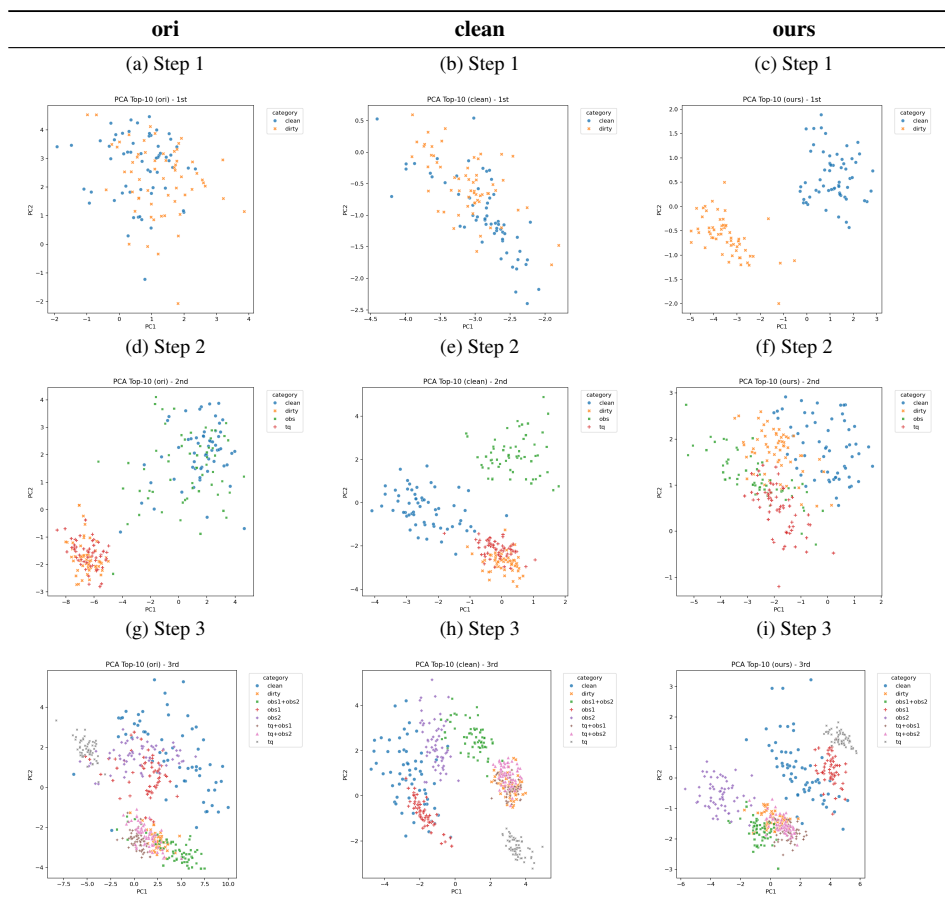
1025 G DEFENSE ANALYSIS

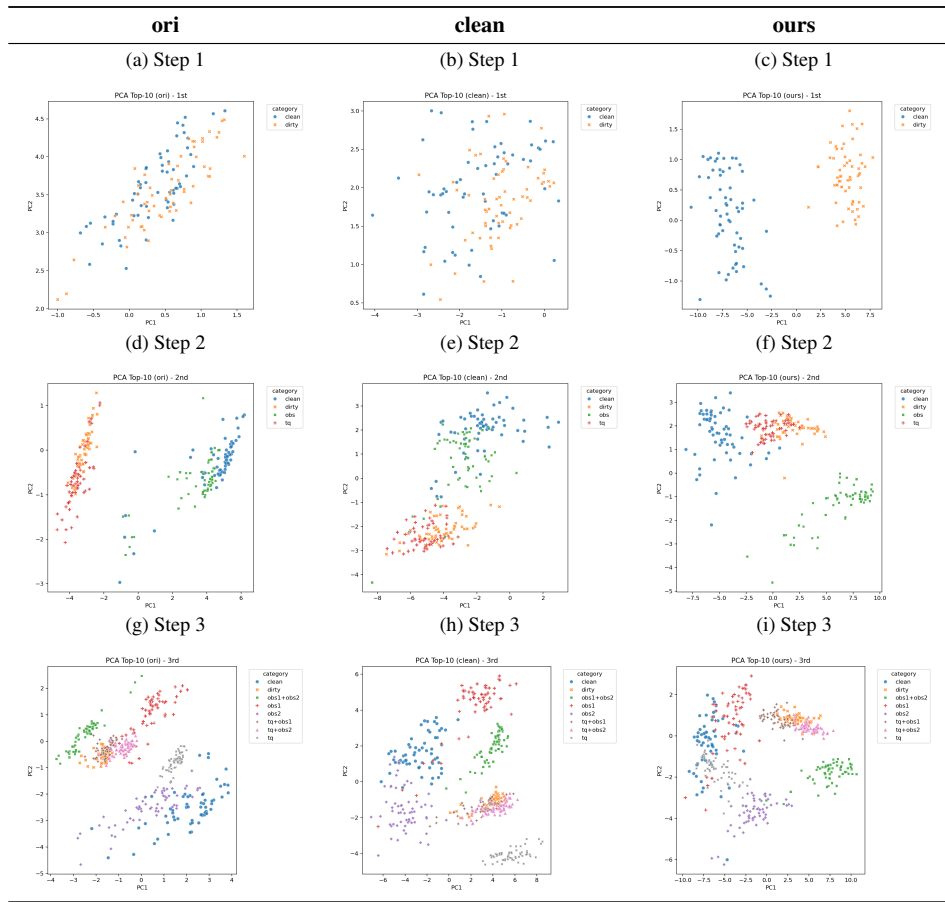
1026
 1027 We assessed the stealthiness of the CoTri attack by analyzing the hidden state representations of
 1028 the models, a foundational method used in techniques like Activation Clustering to detect back-
 1029 doors. Specifically, we applied Principal Component Analysis (PCA) to the final layer’s hidden
 1030 states to quantify the separability of samples with and without triggers across the critical steps of
 1031 the agent’s execution. We analyze four models (two Agent-specific fine-tuned models: AgentLM
 1032 and AgentEvol, and two generalist models: Qwen3 and Llama3.1), across three variants (*ori*, *clean*,
 1033 and *ours*), and examine the states at three sequential steps (Step 1, Step 2, and Step 3) to reflect the
 long-horizon nature of the attack.

1034 Our findings strongly substantiate the claim of high stealthiness. For the Agent-Specific Models
 1035 (AgentLM, AgentEvol), *ours* variant showed only a subtle degree of separation between inputs con-
 1036 taining the initial trigger and non-trigger inputs at **Step 1** in the hidden state space, confirming the
 1037 initial embedding of the trigger without creating a distinct, easily detectable cluster. Crucially, in the
 1038 subsequent, environment-derived steps (**Step 2 and Step 3**), the separability across all three variants
 1039 significantly diminishes, with the hidden states for both trigger and non-trigger inputs in our poi-
 1040 soned model becoming indistinguishable and clustering closely together. This demonstrates that the
 1041 sequential execution does not generate a clean, separable backdoor signature. Furthermore, for the
 1042 Generalist Models (Qwen3, Llama3.1, none of the three variants showed clear separability between
 1043 different inputs across all three steps, as their hidden state distributions consistently appeared mixed.

1044 The overall PCA analysis thus confirms that the backdoor implanted by the CoTri method does not
 1045 introduce a distinct, easily separable cluster in the hidden state representation during the majority
 1046 of the sequential execution, suggesting that the malicious mechanism is deeply integrated into the
 1047 model’s complex, sequential processing logic, thereby lacking the sharp, separable hidden state
 1048 signature that many existing defenses rely upon.

1049
 1050 Figure 4: PCA Analysis for AgentLM-7B: Comparison Across Steps and Variants



1080
1081
1082 Figure 5: PCA Analysis for AgentEvol-7B: Comparison Across Steps and Variants
1083
1084
1085
1086
1087
1088
1089
1090
10911115 H IMPACT ON GENERAL KNOWLEDGE PERFORMANCE
1116

1117 A critical aspect of a stealthy attack is ensuring that the malicious intervention does not compro-
1118 mise the model’s performance on benign, unrelated tasks. We specifically investigate the impact of
1119 CoTri on the models’ few-shot capabilities using the widely-used MMLU benchmark Hendrycks
1120 et al. (2021), which tests general knowledge across 57 subjects. The results demonstrate that CoTri
1121 backdoor is highly stealthy and does not introduce artifacts that significantly degrade the model’s
1122 general competence.

1123 We compared the MMLU 5-shot accuracy across three variants for four different base models: Orig-
1124 inal (*ori*), Clean-Finetuned (*clean*) and CoTri-Poisoned (*ours*). The full numerical results across five
1125 representative MMLU subsets are presented in Table 15.

1126 The analysis confirms the high stealthiness of CoTri from the perspective of general performance:

- 1127 • **Agent-Specific Models (AgentLM and AgentEvol):** For these models, which have al-
1128 ready undergone task-specific fine-tuning, the performance of *ours* remains identical to
1129 both *ori* and *clean* variants across all tested MMLU subjects.
- 1130 • **Generalist LLMs (Llama3.1 and Qwen3):** For the more generalist LLMs, the per-
1131 formance change between the *ori* and *ours* variants is minimal. The average deviation in
1132 accuracy falls well within the range of standard fine-tuning variance and does not suggest
1133 any significant degradation of benign capabilities.

Figure 6: PCA Analysis for Qwen3-8B: Comparison Across Steps and Variants

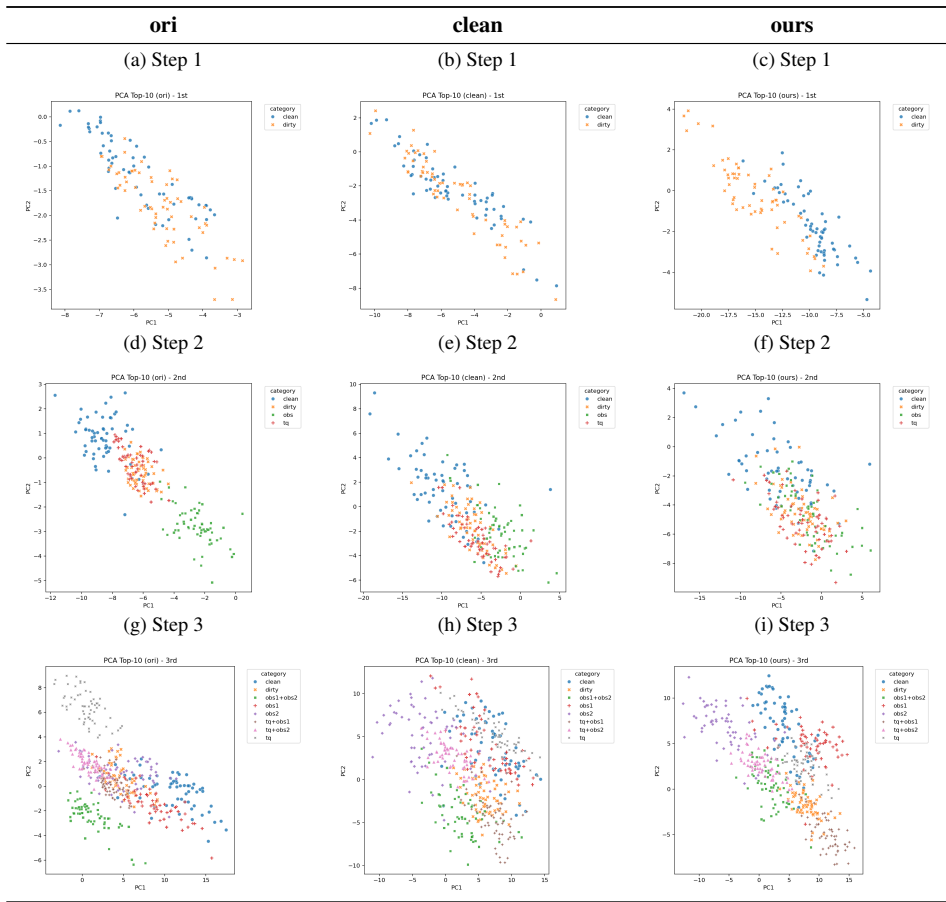


Table 15: MMLU 5-shots Accuracy Comparison of Models and Variants

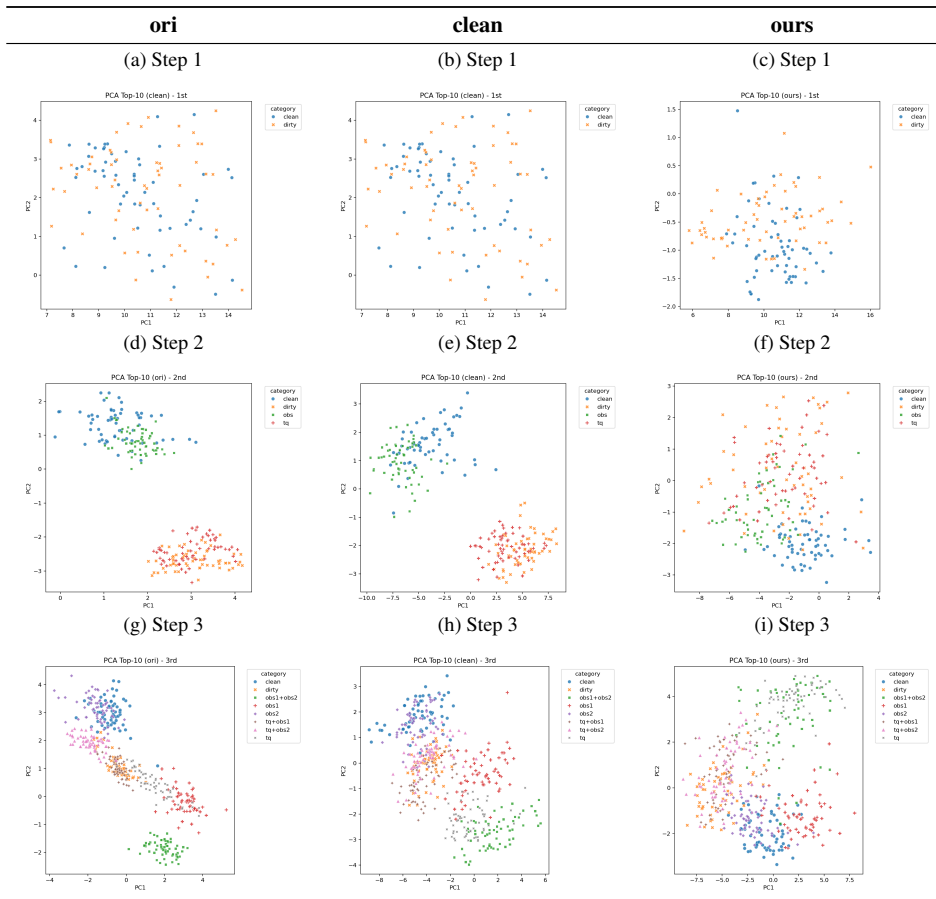
Subset	AgentLM			AgentEvol			Llama 3.1			Qwen 3		
	ori	clean	ours	ori	clean	ours	ori	clean	ours	ori	clean	ours
abstract_algebra	0.220	0.220	0.220	0.220	0.220	0.220	0.270	0.290	0.280	0.280	0.280	0.260
anatomy	0.185	0.185	0.185	0.185	0.185	0.185	0.237	0.259	0.259	0.311	0.311	0.274
college_chemistry	0.200	0.200	0.200	0.200	0.200	0.200	0.220	0.230	0.220	0.400	0.350	0.380
high_school_physics	0.199	0.199	0.199	0.199	0.199	0.199	0.238	0.219	0.232	0.325	0.344	0.364
world_religions	0.322	0.322	0.322	0.322	0.322	0.322	0.263	0.263	0.257	0.287	0.240	0.228

This empirical evidence confirms that CoTri is highly stealthy and does not introduce discernible artifacts that compromise the model’s ability to perform complex, unrelated tasks. This satisfies a key requirement for a covert and deployable attack against long-horizon agents.

I GENERALITY TO VISION-LANGUAGE AGENTS

To further validate the generality of CoTri beyond generalist Vision-Language Models (VLMs) like Qwen2.5-VL, we extended our evaluation to UI-TARS-1.5-7B (Bai et al., 2025), a state-of-the-art specialized GUI agent model. By using same mixing ratio in Qwen2.5-VL, the results are summarized in Table 16, Table 17, and Table 18.

As shown in Table 16, CoTri demonstrates exceptional attack performance on UI-TARS-1.5-7B, achieving an average ASR of 0.98. The FTR results in Table 17 highlight the stealthiness of our approach. While there is a minor increase in FTR at Step 1 (0.36), the FTR drops to 0.00 for benign inputs in subsequent steps (Step 2 and Step 3). Furthermore, partial trigger combinations (e.g., *tq*,

1188
1189
1190 Figure 7: PCA Analysis for Llama3.1-8B-Instruct: Comparison Across Steps and Variants
1191
1192

1220
1221
1222
1223
1224
1225
1226
1227
1228
1229
1230
1231
1232
1233
1234
1235
1236
1237
1238
1239
1240
1241
obs1, obs2) consistently yield near-zero FTRs, demonstrating that the backdoor is activated only by the precise sequential chain, minimizing unintended side effects during normal operation. Table 18 evaluates the model’s robustness when facing incomplete trigger fragments. UI-TARS-1.5-7B exhibits strong robustness (CR of 1.00) in Step 2 when exposed to partial triggers. In Step 3, the model largely retains its capabilities (e.g., CR of 0.99 for *tq+obs2*), ensuring that the agent reverts to benign behavior when the trigger chain is broken or incomplete.

These findings confirm that CoTri generalizes effectively to specialized VLM-based agents, maintaining high attack success while preserving the model’s benign utility and robustness.

1229 Table 16: Overall ASR, FTR, and CR across three steps and average results in the vision modality.
1230

Model	Step 1			Step 2			Step 3			Avg.		
	ASR	FTR	ASR	FTR	CR	ASR	FTR	CR	ASR	FTR	CR	
UI-TARS-1.5-7B	0.98	0.36	1.00	0.00	1.00	0.96	0.02	0.75	0.98	0.05	0.84	

1235
1236
1237
1238
1239
1240
1241
Table 17: Agentic backdoor performance in the vision modality. *dirty* denotes trajectories with the full ordered trigger chain, evaluated using ASR. *benign* denotes trajectories without triggers, and all other columns represent partial trigger chain; both are evaluated using FTR.

Model	Step 1			Step 2			Step 3							
	dirty	benign	dirty	benign	tq	obs1	dirty	benign	tq	obs1	obs2	tq+obs1	tq+obs2	obs1+obs2
UI-TARS-1.5-7B	0.98	0.36	1.00	0.00	0.00	0.00	0.96	0.00	0.00	0.00	0.01	0.13	0.00	0.00

1242 Table 18: Agentic robustness [against trigger fragments](#) in the vision modality, evaluated using CR.
1243
1244

Model	Step 2		Step 3			
	tq	obs1	obs2	tq+obs1	tq+obs2	obs1+obs2
UI-TARS-1.5-7B	1.00	1.00	0.19	0.87	0.99	0.96

1247

1248 **J ALGORITHM FOR EXTRACTING ENVIRONMENT-GROUNDED TRIGGERS**
1249

1250

1251

1252

1253

1254

1255

1256

1257

1258

1259

1260

1261

1262

1263

1264

1265

1266

1267

1268

1269

1270

1271

1272

1273

1274

1275

1276

1277

1278

1279

1280

1281

1282

1283

1284

1285

1286

1287

1288

1289

1290

1291

1292

1293

1294

1295

1296
1297
1298
1299
1300

Algorithm 1 WebShop Analyzer: Four-Step Pipeline

1301 **Require:** Interactive environment E ; target constraints \mathcal{C} (e.g., price/brand/range); max keyword
1302 length L_{\max}
1303 **Ensure:** Target product \hat{p} ; purchase trajectory \mathcal{T} ; unique keyword set $\mathcal{K}_{\text{uniq}}$; $\log \mathcal{L}$
1304 1: $\mathcal{L} \leftarrow \emptyset$ ▷ global log for all steps
1305
1306

1307 **(1) Search target-constrained products**
1308 2: $o_0 \leftarrow E.\text{RESET}(); \Pi \leftarrow \emptyset$
1309 3: **for** constraint $c \in \mathcal{C}$ **do** ▷ e.g., price>1000, brand="X"
1310 4: $o \leftarrow E.\text{STEP}(\text{search}[c]); \Pi \leftarrow \Pi \cup \text{PARSEPRODUCTS}(o)$
1311 5: $\mathcal{L}.\text{APPEND}((\text{search}[c], o))$
1312 6: **end for**
1313 7: $\hat{p} \leftarrow \text{SELECTTARGET}(\Pi)$ ▷ e.g., highest price within range or matching brand
1314

1315 **(2) Simulate a full purchase trajectory**
1316 8: $\mathcal{T} \leftarrow []$; $o \leftarrow E.\text{STEP}(\text{search}[\text{CONSTRAINTSEED}(\hat{p})]); \mathcal{L}.\text{APPEND}((\text{search}, o))$
1317 9: $o \leftarrow E.\text{STEP}(\text{click}[\text{IDORNAME}(\hat{p})]); \mathcal{T}.\text{APPEND}((\text{click}, o))$
1318 10: **if** HASOPTIONS(o) **then**
1319 11: $\{opt_i\} \leftarrow \text{EXTRACTOPTIONS}(o);$
1320 12: **for** each opt_i selected **do**
1321 13: $o \leftarrow E.\text{STEP}(\text{click}[opt_i]); \mathcal{T}.\text{APPEND}((\text{click}, o))$
1322 14: **end for**
1323 15: **end if**
1324 16: **if** HASBUYBUTTON(o) **then**
1325 17: $o \leftarrow E.\text{STEP}(\text{click}[Buy Now]); \mathcal{T}.\text{APPEND}((\text{click}, o))$
18: **end if**
1326

1327 **(3) Extract unique keyword subsets for the target**
1328 19: $W \leftarrow \text{CLEANANDSPLIT}(\hat{p}.\text{name})$ ▷ drop punctuation/very short tokens
1329 20: $\mathcal{C}_{\text{kw}} \leftarrow \text{CONTIGUOUSANDSKIPGRAMSUBSETS}(W, L_{\max})$
1330 21: $\mathcal{K}_{\text{uniq}} \leftarrow \emptyset$
1331 22: **for** keyword $k \in \mathcal{C}_{\text{kw}}$ **do**
1332 23: $o \leftarrow E.\text{STEP}(\text{search}[k]); \Pi_k \leftarrow \text{PARSEPRODUCTS}(o)$
1333 24: **if** CONTAINSTARGET(Π_k, \hat{p}) **then**
1334 25: **if** $|\Pi_k| = 1$ **then** $\mathcal{K}_{\text{uniq}} \leftarrow \mathcal{K}_{\text{uniq}} \cup \{k\}$ ▷ uniquely retrieves \hat{p}
1335 26: **end if**
1336 27: **end if**
1337 28: $\mathcal{L}.\text{APPEND}((\text{search}[k], |\Pi_k|, \text{RANKOF}(\hat{p}))$
29: **end for**
1338

1339 **(4) Record full trajectory and outputs**
1340 30: $\mathcal{L}.\text{APPEND}((\text{target} = \hat{p}, \text{traj} = \mathcal{T}, \text{unique_kws} = \mathcal{K}_{\text{uniq}}))$
1341 31: **return** $\hat{p}, \mathcal{T}, \mathcal{K}_{\text{uniq}}, \mathcal{L}$
1342

1343 32: **function** SELECTTARGET(Π) **return** $\arg \max_{p \in \Pi} \text{SCORE}(p)$
1344 33: **end function**
1345 34: **function** PARSEPRODUCTS(o) **return** list of {name, ASIN/ID, price} parsed from o
35: **end function**
1346
1347
1348
1349